NPS ARCHIVE
1965
BURCHER, P.

THE APPLICATION OF DYNAMIC POLARIZATION TO EARTH'S FIELD NUCLEAR RESONANCE MAGNETOMETERS

PHILIP E. BURCHER
RAYMOND G. LANDRUM

DUDLEY KNOX LIBRARY
NAVAL POSTGRADUATE SCHOOL
MONTEREY, CA 93943-5101

64

THE APPLICATION OF DYNAMIC POLARIZATION TO EARTH'S FIELD NUCLEAR RESONANCE MAGNETOMETERS

* * * * *

Philip E. Burcher

and

Raymond G. Landrum

THE APPLICATION OF DYNAMIC POLARIZATION TO EARTH'S FIELD NUCLEAR RESONANCE MAGNETOMETERS

by

Philip E. Burcher

Lieutenant, United States Navy

and

Raymond G. Landrum

Lieutenant, United States Navy

Submitted in partial fulfillment of
the requirements for the degree of

MASTER OF SCIENCE

IN

ENGINEERING ELECTRONICS

United States Naval Postgraduate School
Monterey, California

1 9 6 5

[illegible]
[illegible]

NPS ARCHIVE
19[illegible]
SCHAEFFER, P

DUDLEY KNOX LIBRARY
NAVAL POSTGRADUATE SCHOOL
MONTEREY, CA 93943-5101

THE APPLICATION OF DYNAMIC POLARIZATION TO EARTH'S FIELD NUCLEAR RESONANCE MAGNETOMETERS

by

Philip E. Burcher

and

Raymond G. Landrum

This work is accepted as fulfilling
the thesis requirements for the degree of
MASTER OF SCIENCE
IN
ENGINEERING ELECTRONICS
from the
United States Naval Postgraduate School

ABSTRACT

The principle of Nuclear Magnetic Resonance has, for many years, been applied to the measurement of the earth's magnetic field. Of the magnetometers based on this principle, the Free Precession Magnetometer gives the best absolute accuracy available today. Disadvantages of this device are its comparatively slow data rate and transients created by the polarizing current pulses. The application of the Overhauser Effect, or Dynamic Polarization, to a nuclear resonance magnetometer offers advantages in increased data rate and accuracy. Such magnetometers have been limited by the short lifetime of the sample material.

Three devices, in which dynamic polarization is used, are described. One of these, a maser oscillator, seems particularly promising. Also included is a study of the requirements for long-lifetime materials suitable for use in a magnetometer.

The authors wish to express their appreciation to Prof. Carl E. Menneken for suggesting the thesis topic and for his advice and encouragement, to Dr. William M. Tolles for his explanations of electron resonance theory and for his assistance in the selection and preparation of samples, to Dr. Gordon E. Schacher for providing a physical interpretation of the Overhauser Effect, and to Mr. Robert A. Anderson for his assistance in the design and construction of the experimental equipment.

TABLE OF CONTENTS

Section		Page
1.	Introduction	1
2.	Nuclear Magnetic Resonance	4
3.	The Free Precession or Proton Magnetometer	8
4.	Electron Paramagnetic Resonance	10
5.	The Overhauser Effect	11
6.	The Maser Oscillator	19
7.	The Experimental System	24
	a. The Modified Free Precession Magnetometer	25
	b. The Maser Oscillator Magnetometer	26
	c. Marginal Oscillator	27
	d. Sample - Detection Coils	31
	e. R. F. Enhancement Coils	34
	f. R. F. Coil Matching	36
	g. Determining the Saturation Factor	39
	h. Sample Materials	41
8.	Experimental Results	56
9.	Conclusions	65
10.	Bibliography	67
Appendix A.	Modulated Field Technique	68
Appendix B.	Sample Preparation	77
Appendix C.	Equipment Circuit Diagrams	79
Appendix D.	Subsidiary Bibliographic Material	83

LIST OF ILLUSTRATIONS

Figure		Page
1.	Typical Free Precession Magnetometer Signal	2
2.	Magnetic Resonance Vector Diagram	4
3.	Plot of Enhancement and Signal vs Saturation Factor	17
4.	Block Diagram - Maser Oscillator	19
5.	Block Diagram - Standard Free Precession Magnetometer	25
6.	Block Diagram - Modified Free Precession Magnetometer	26
7.	Simplest Marginal Oscillator	28
8.	Block Diagram - Phase Shift Oscillator	29
9.	Block Diagram - Band Pass Amplifier/Oscillator	30
10.	Marginal Oscillator in Final Form	31
11.	Dual Detection Coil Arrangement	33
12.	Detection Coil	34
13.	R. F. Coil Matching Network	36
14.	Impedance Matching Loci	38
15.	Derivative of Electronic Resonance Absorption vs Magnetic Field for Peroxylamine Disulfonate	45
16.	Calculated Low Field Energy Level Diagram for Peroxylamine Disulfonate Model	47
17.	Vector Representation of Quantum Numbers	48
18.	Frequency vs Field Strength for Allowed Transition in Peroxylamine Disulfonate Model	50
19.	Transition Probability vs Field Strength for Peroxylamine Disulfonate Model	51
20.	Line Intensity vs Frequency at H = 15 Gauss for DPPH and $(SO_3)_2NO^{--}$	52
21.	Low Field Energy Level Diagram for DPPH Model	54
22.	Signal from Modified Free Precession Magnetometer	56

Figure Page

23. Comparison of Normal and Dynamic Polarization 57

24. Signal Amplitude vs Polarizing Field for Peroxylamine Disulfonate 59

25. Variation in Signal Period with Time 62

26. Direct Recording of Maser Oscillator Frequency 63

27. Modulated Field Absorption 68

28. Block Diagram - Modulated Field System 69

29. Helmholtz Sweep Coils 70

30. Helmholtz Coil Driver 71

31. The Relaxation Time of the Proton Resonance in Aqueous Solutions of Paramagnetic Salts 72

LIST OF SYMBOLS

$\vec{a}$	Angular momentum
c	Velocity of light = 3×10^{8} m/sec
e	Charge on the electron = 1.6×10^{-19} coulombs
f	frequency
$\hbar$	Planck's Constant/2π = 1.05×10^{-27} erg-sec
k	Boltzmann's Constant = 1.38×10^{-23} joules/°K
m_e	electron mass = 9.1×10^{-31} Kg
m_p	proton mass = 1.67×10^{-27} Kg
$n_{+,-}$	electron energy level population
s	saturation factor
s'	saturation parameter
w	lattice induced transition probability
$\vec{A}$	resultant angular momentum
A	hyperfine coupling constant
E	energy
H	ambient magnetic field
H_0	D. C. magnetic field
H_1	R. F. magnetic field
$\vec{I}$	nuclear spin
$\vec{M}$	resultant magnetic moment
M_0	D. C. magnetic moment
$N_{+,-}$	nuclear energy level population
Q	quality factor
$\vec{S}$	electron spin
T	temperature, °K
$\vec{T}$	total torque
T_1	longitudinal relaxation time

T_2	transverse relaxation time
W	R. F. induced transition probability
Δ, δ	change in
γ	gyromagnetic ratio $\gamma/2\pi = 4.2576$ KC/gauss
η	filling factor
ρ_1	signal-to-noise ratio
Γ	units of magnetic field strength, gamma $1\Gamma = 10^{-5}$ gauss
τ	measurement interval
$\vec{\mu}$	magnetic moment
μ_B, μ_e	Bohr Magneton $= 9.27 \times 10^{-21}$ erg/gauss
μ_n	nuclear magneton $= 1.41 \times 10^{-23}$ erg/gauss
ω	angular frequency
$\vec{\omega}_0$	angular precession frequency
a	enhancement signal magnitude
a_0	unenhanced signal magnitude
$\mathcal{T}$	magnetic dipole-dipole interaction tensor

1. Introduction.

For a number of years, the measurement of the direction, magnitude and changes in magnitude of the earth's magnetic field has been of interest to the geophysicist, the magnetic prospector and to the military in the fields of anti-submarine warfare and mine countermeasures. The devices used to measure one or more of the properties of the earth's field are known as magnetometers. The types of magnetometers cover a broad spectrum, ranging in complexity from a simple dip needle, through equipments such as the flux gate magnetometer, to the more exotic rubidium vapor and metastable helium devices. Depending on the application, magnetometers may be found in fixed station installations, in vehicles and aircraft and, for the past few years, in satellites and space probes. Magnetometers are as diverse as the uses to which they are put, each having its own characteristics, advantages and disadvantages which suit it to a particular application.

One type of magnetometer which has found wide use due to its simplicity and measurement accuracy is the proton or free precession magnetometer [4]. This type of magnetometer, which will be discussed in more detail in a later section, utilizes the phenomenon of nuclear or proton magnetic resonance. It consists primarily of a coil surrounding a sample of material, such as ordinary water, that contains a large number of protons. The sample is polarized by a magnetic field created by passing a DC current through the coil. The field is then suddenly cut off and the protons allowed to precess about the earth's field. The precession frequency is directly proportional to the magnitude of the earth's field and the free precession magnetometer measures the magnitude of the field by accurately measuring the proton precession frequency.

The output of this type of magnetometer is not continuous but takes the form of a damped sinusoid as shown in Fig. 1.

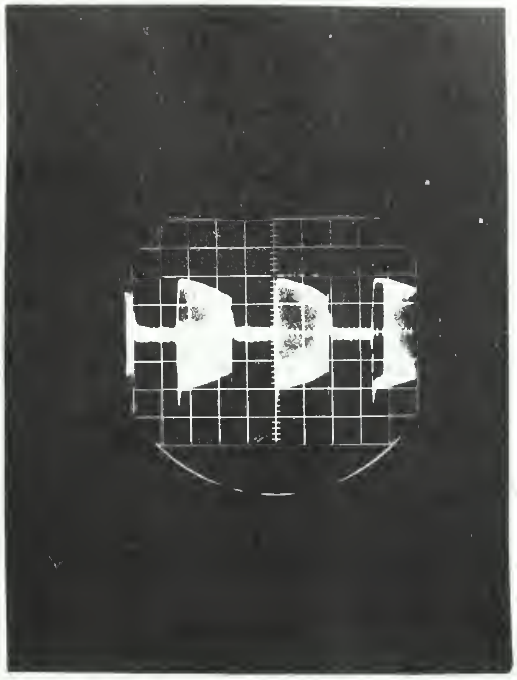

Typical Free Precession Magnetometer Signal

Figure 1.

The time available for measurement of the precession frequency depends on the time constant of the decaying signal and on the initial signal magnitude, which is related to the duration of the polarizing signal. This measurement time is on the order of 1-2 seconds. A typical polarize-measure cycle takes 4-5 seconds. Therefore the proton magnetometer is characterized by a relatively low data rate, a severe limitation in certain mobile applications.

Several techniques have been utilized to increase the data rate. These include the use of two magnetometers in a time-sharing scheme [6]. Improvements in signal-to-noise ratio have been achieved primarily by circuit design techniques aimed at reducing circuit noise. A technique

which not only allows continuous measurements to be made, thereby eliminating the data rate problem, but also provides a significant improvement in the signal to noise ratio, is the technique of dynamic polarization or the Overhauser Effect. Dynamic polarization takes advantage of the coupling that exists between free electrons and protons to enhance the polarization of the protons thereby improving the signal-to-noise ratio. Magnetometers utilizing this technique have been built and have given good measurement accuracy but, for the most part, have been useful only as laboratory instruments due to the short lifetimes of the materials used as samples.

The purpose of this study is to describe the construction and operation of a magnetometer based on the principle of dynamic polarization and to investigate materials having a sufficient lifetime so as to be useful in a practical magnetometer.

2. Nuclear Magnetic Resonance.

The phenomenon of nuclear magnetic resonance is possible due to the fact that some atomic nuclei possess both angular momentum and magnetic moments. These nuclei, for example the protons found in ordinary water, may be thought of as being tiny magnetized gyroscopes, each having a magnetic moment $\vec{\mu}$ and an angular momentum $\vec{a}$ which are colinear. Under the influence of an applied static magnetic field, a sample of material, such as water, containing an ensemble of N nuclei will exhibit a resultant magnetic moment $\vec{M}=\overline{N}\vec{\mu}$ ($\overline{N}$ is the average number of nuclei) and a resultant angular momentum $\vec{A}=\overline{N}\vec{a}$ as shown in Fig. 2 [10] . Like a gyroscope acted upon by the force of gravity, the magnetic moment vector

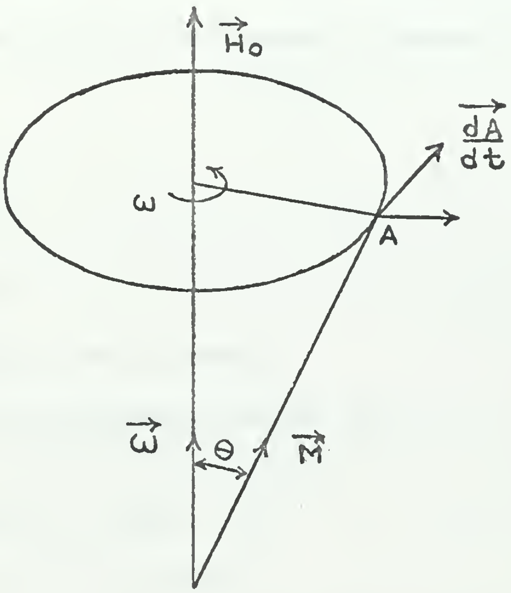

Magnetic Resonance Vector Diagram

Figure 2.

$\vec{M}$ will precess about the applied field vector $\vec{H}_o$ at a frequency that is directly proportional to H_o. This angular precession frequency is known as the Larmor frequency.

From conservation of angular momentum:

$$\frac{d\vec{A}}{dt} = \vec{T} = \text{total torque}$$

and $\vec{T} = \vec{M} \times \vec{H}_0$.

Also; $\frac{d\vec{A}}{dt} = \omega_0 \times \vec{A}$.

Therefore $\vec{M} \times \vec{H}_0 = \vec{\omega}_0 \times \vec{A}$ or $M H_0 \sin\theta = \omega_0 A \sin\theta$. Finally, $\omega_0 = \left(\frac{M}{A}\right) H_0$, an expression relating the precession frequency to the magnitude of the applied field. The ratio $\left(\frac{M}{A}\right)$ is known as the "gyromagnetic ratio", given the symbol γ , and is a constant for a particular nucleus, independent of all experimental conditions. Thus, for a given nucleus, there is a precession frequency corresponding to a given value of applied magnetic field.

The above relation can also be derived using quantum mechanics. In quantum mechanics the unit for magnetic moments is the Bohr Magneton:

$$\mu_B = \frac{e\hbar}{2m_e c} ,$$

where

e = charge on an electron,

$\hbar$ = Planck's constant divided by 2 ($\hbar = 1.05 \quad 10^{-27}$ erg-sec),

c = velocity of light and

m_e = mass of the electron.

The nuclear magneton is related to the Bohr magneton by the ratio of the mass of the proton to the mass of the electron, the nuclear magneton being:

$$\mu_n = \frac{e\hbar}{2 m_p c}$$

The theoretical value of μ_n for protons is 5.0505×10^{-24} erg/gauss. However, precise measurements of μ_n have shown it to be 2.79268 times the theoretical value, giving a value of 1.41×10^{-23} erg/gauss [1].

When a nucleus having spin, or an electron, is placed in a magnetic field a splitting of the energy level occurs known as the Zeeman Effect. The difference in energy E between the Zeeman levels is given by:

$$E = \frac{\mu H_0}{I} = \omega_0 \hbar$$

where, I = nuclear spin and, for protons, has the value 1/2. Transposing,

$$\omega_0 = \frac{\mu}{I\hbar} H_0 = \left(\frac{2\mu}{\hbar}\right) H_0$$

the quantity $\left(\frac{\mu}{I\hbar}\right)$ being the gyromagnetic ratio, γ .

Therefore,

$$f_0 = \frac{\gamma}{2\pi} H_0 \quad .$$

For protons, $\frac{\gamma}{2\pi} = 4.2576$ KC/gauss, giving for the earth's magnetic field ($\approx .5$ gauss) a precession frequency of about 2KC.

When a magnetic field is applied to a substance containing nuclei with magnetic moments, the magnetic moment vectors align both parallel and anti-parallel to the applied field. The majority align with the field giving a net magnetic moment vector, $\vec{M}$. The magnetic moment vector approaches alignment exponentially with a time constant T_1 , the longitudinal relaxation time. If the applied field is removed, the moment vector departs from alignment exponentially with a time constant T_2 , the transverse relaxation time.

The important points to remember concerning nuclear magnetic

resonance are:

(1) that for a given nucleus, there is a precession frequency corresponding to a given magnitude of applied magnetic field,

(2) that there is a net alignment of the magnetic moment vectors with the applied field, and

(3) that these vectors approach and depart from alignment in an exponential manner.

3. The Free Precession or Proton Magnetometer.

Although the free precession magnetometer is not the primary subject of this thesis, a brief discussion of its characteristics is considered a necessary prerequisite for an understanding of the magnetometer based on the Overhauser Effect.

As stated in Section 1, the free precession magnetometer consists primarily of a coil surrounding a sample of material which contains a large number of protons. It should be pointed out that materials other than water, kerosene for instance, are used as samples, but in this discussion ordinary water will be used as an example.

In the proton magnetometer, a DC current, of sufficient magnitude to create a magnetic field in the sample roughly 200 times greater than the earth's field, is passed through the coil surrounding the water sample. This polarizing field is applied for a time approximately equal to $5T_1$ and then is suddenly cut off. During the time the polarizing field is on, the resultant magnetic moment vector $\vec{M}$ will precess about $\vec{H}_o$, gradually coming into alignment with it. When the polarizing field is removed the magnetic moment vector precesses about the only remaining field, that of the earth, at a frequency directly proportional to the magnitude of the earth's field. The applied field must be removed in such a manner that the resultant magnetic moment vector does not follow it. Due to the precessional motion, a voltage of a few microvolts magnitude is induced in the magnetometer coil. Because the magnitude of the magnetic moment vector is decreasing exponentially, the signal induced in the coil is an exponentially decreasing sinusoid, as shown in Fig. 1. This voltage is amplified and its frequency is measured to determine the magnitude of the earth's field.

The accuracy of the proton magnetometer in determining the value

of the earth's field depends on the accuracy with which one can measure the frequency of the output voltage. Generally, the longer the time available for measurement, the greater the accuracy will be. This available measuring time is in turn dependent on the rate at which the output signal decays and on its initial magnitude; the signal ceases to be useable when it decays below the circuit noise level. Also, sufficient time must be allowed for switching transients to decay prior to starting the measurement. Assuming proper circuit design, the decay rate is determined only by the characteristics of the sample being used and is not controllable. Again, assuming proper circuit design, the initial magnitude of the signal is determined by the initial magnitude of the resultant magnetic moment vector, $\vec{M}$.

When the sample is polarized not all the nuclear magnetic moments are aligned to form the resultant vector. In this type of magnetometer, the number of nuclear magnetic moments polarized can be increased only by increasing the magnitude and/or duration of the applied field. Since no data is received during the polarizing period, use of this technique serves only to decrease an already slow data rate. If the polarizing time is decreased, the measurement time and, as a result, the accuracy are reduced.

In summary, the standard free precession magnetometer is characterized by a slow data rate which can be increased only at the expense of accuracy. The accuracy obtained depends on the measurement time which is determined by the initial signal magnitude and rate of decay.

As will be shown, the magnetometer based on the Overhauser Effect not only eliminates the data rate problem by giving a continuous output signal but also increases the magnitude of that signal.

4. Electron Resonance.

Like the proton, the electron also has a magnetic moment and angular momentum. In the presence of a magnetic field, it too will exhibit the resonance phenomenon. The angular precession frequency of the electron is, however, much higher than that of the proton.

Recall that the angular precession frequency is directly proportional to the gyromagnetic ratio and inversely proportional to the mass of the particle, i.e. $\omega \propto \gamma \propto 1/m$. As an example, for protons and free electrons, the mass of the electron is approximately 1/1836 that of the proton. The electron resonance frequency will thus theoretically be 1836 times that of the proton for a given value of magnetic field. As pointed out in Section 2, the observed magnetic moment of the proton is 2.7927 times the theoretical value. Thus the ratio of electronic resonance frequency to that of the proton is actually 660. In the earth's field the proton frequency has been shown to be about 2 KC; the electron frequency will be in the megacycle range.

A major difference in nuclear and electronic resonance properties is the effect of the surroundings. In electron resonance there is a very strong electrostatic interaction with the lattice, while in nuclear resonance the electrons tend to shield the nucleus from the surroundings. The electron resonance observed for an atom in a crystal lattice and for the same atom in a liquid solution may be expected to differ markedly. This difference becomes important to the study of Overhauser Effect in free radical solutions which is discussed in Section 5.

5. The Overhauser Effect.

Dynamic polarization or Overhauser Effect was first described by Albert W. Overhauser in a paper [2] published in February 1953. This original article conceived the effect only as applied to metals. Extension of the theory to non-metals was carried out by A. Abragam in an article published in June 1955 [5]. The verification of the Overhauser Effect was carried out by various investigators, first by Carver and Slichter whose results were published in May, 1956 [7].

The arguments which follow in describing the Overhauser Effect are a basic application of the principles of statistical mechanics. They include only as much as is needed to describe the phenomen plausibly. For a more complete treatment reference may be made to the original papers above or to Abragam [14].

Assume a spin system in thermal equilibrium with a reservoir (lattice) at a temperature, T. The derivation is based upon the general theorem of statistical mechanics which states that the relative populations at two energy levels, assuming Boltzman statistics apply, is given by

$$\frac{N_-}{N_+} = e^{-\frac{\Delta E_R}{RT}}$$

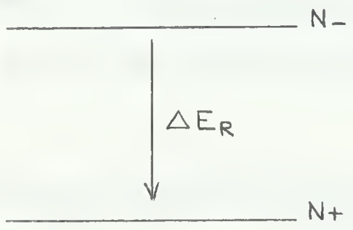

where $N_{+,-}$ represent populations at the levels shown (N_+ refers to spins aligned with the external magnetic field and N_- to those anti-aligned) and ΔE_R is the energy change of the reservoir when a particle makes a transition from a level represented by N_- to a level represented by N_+ .

For an isolated nuclear spin system in an external field, H_o ,

$$\Delta E = 2|\mu_n| H_o ,$$

where $\mu_n =$ the magnetic moment of the nuclei. Then and the relative population is given by

$$\frac{N-}{N+} = e^{-2|\mu_n| H_o/kT} .$$

Since for normal experimental conditions, $|\mu_n| H_o << kT$, one may write

$$\frac{N+}{N-} \approx 2|\mu_n| H_o/kT$$

This is normally referred to as the high temperature approximation.

If coupling exists between the electronic and nuclear spin systems, the interaction with electrons must be included. Nuclei have weak coupling with the lattice whereas electrons have strong spin-lattice coupling. Therefore, since nuclei exhibit strong coupling with electrons, the nuclei stay in thermal equilibrium with the lattice via interaction with electrons.

Assume that the electron-nuclear interaction is given by the hyperfine interaction:

$$A \vec{I} \cdot \vec{S} = A(I_x S_x + I_y S_y + I_z S_z) \qquad (1)$$

where A = the hyperfine coupling constant (assumed present in the derivation which follows). In order to rewrite equation (1), use the vector operators:

$I_+ = I_x + jI_y$ is a quantum mechanical operator which when operating on the wave function describing the spin system with N_+ and N_- converts it to a wave function with $N_+ + 1$ and $N_- - 1$. (i.e. a raising operator)

$I_- = I_x - jI_y$ is a lowering operator (i.e. it takes N_+, N_- to $N_+ - 1$, $N_- + 1$).

$j = \sqrt{-1}$

In the same manner the operators S_+ and S_- are defined. Substituting into (1) gives

$$\vec{I} \cdot \vec{S} = I_z S_z + \frac{1}{2}(I_+ S_- + I_- S_+)$$

For this electron-nuclear system the energy levels will appear as shown in the following diagram.

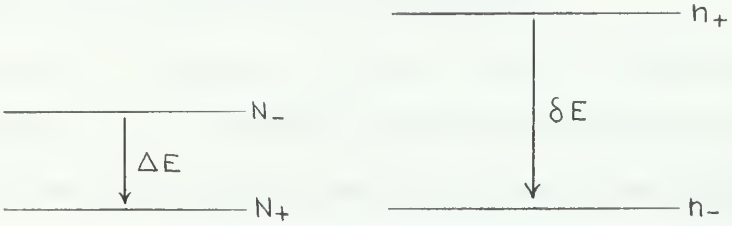

Here the electronic populations are designated by $n_{+,-}$ and δE is given by

$$\delta E = 2|\mu_e| H_0$$

Note that the electronic energy levels are inverted with respect to the nuclear energy levels since the electron has negative sign.

Recognizing that the nuclei are decoupled from the lattice it is apparent that nuclear transitions must be accompanied by electronic

transitions. The possible transitions are given by the hyperfine interaction terms $I_+ S_-$, $I_- S_+$ and $I_z S_z$. $I_z S_z$ is of no interest since it represents no transitions. The other two terms indicate that nuclear transitions must be accompanied by electronic transitions in the opposite direction. Thus for nuclear spin to make a transition from N_- to N_+, ΔE_R must be

$$\Delta E_R = 2|\mu_n| H_0 + 2|\mu_e| H_0$$

(Such a transition is shown on the preceeding page). In calculating the N_+ to N_- ratio one must consider the state of the system after only the nuclear population is changed. The electronic spin relaxes back to its original level through lattice interaction leaving the net result that

$$\Delta E_R(\text{net}) = 2|\mu_n| H_0$$

as before, and the population ratio is unchanged.

Now assume that a strong r.f. field is applied at the electron resonance frequency, ω_e, such that the electronic transition probability caused by the r.f. field is very much greater than that caused by lattice interactions. Then the electron spin is relaxed back to its original state by absorption of energy from the r.f. field with the result that the total energy change of the reservoir for the whole process is

$$\Delta E_R(\text{net}) = 2|\mu_n| H_0 + 2|\mu_e| H_0 .$$

The high temperature approximation gives

$$\frac{N_+}{N_-} \approx 2|\mu_n| H_0 + 2|\mu_e| H_0 \qquad (2)$$

Since $|\mu_e|/|\mu_n| = 657$ (for protons and free electrons) the population difference $(N_+ - N_-)$ is seen to be greatly enhanced on the application of a r.f. field. In a nuclear resonance experiment the observed signal is proportional to the population difference, so that the application of a r.f. field tends to greatly enhance the nuclear resonance signal. It is common to define enhancement by:

$$\mathcal{E} = \frac{a - a_0}{a_0} \tag{3}$$

where a = the enhancement signal magnitude and a_0 = the unenhanced signal magnitude. Substituting into equation (2) immediately gives

$\mathcal{E} \approx 657$ for protons and free electrons.

This effect is commonly referred to as Overhauser Effect.

In the experiments reported in this paper, equation (1) does not apply for the electron-nuclear interaction. The correct interaction is magnetic dipole-dipole interaction represented by

$$\vec{I} \cdot \mathcal{J} \cdot \vec{S} \, ,$$

where $\mathcal{J}$ is a tensor. This interaction may be rewritten as before leading to the following possible transitions:

1) $I_+ S_-$, $I_- S_+$
2) $I_- S_-$, $I_+ S_+$
3) $I_+ S_z$

Let f_1, f_2, and f_3 be the relative probabilities that these transitions occur. $(f_1 + f_2 + f_3 = 1)$.

Further, relax the restriction that the r.f. induced electronic transition probabilities be very much greater than lattice induced transition probabilities. Define the saturation factor, s,

$$S \overset{D}{=} \frac{W}{\omega}$$

where W is the r.f. induced transition probability and ω is the lattice induced transition probability. Overhauser has shown [3] that

$$S = \gamma_e^{2} H_1^{2} T_1 T_2 .$$

Note that $\frac{S}{S+1}$ = the fraction of electron spins relaxed by the r.f. field. Proceeding in a fashion analagous to that preceeding for hyperfine interaction gives

$$\frac{N_-}{N_+} = e^{-2(|\mu_n| + \frac{S}{S+1}(f_2 - f_1)|\mu_e|)H_0/kT .}$$

For dipolar coupling in liquids the transition probabilities are approximately $f_1 = 0.1$, $f_2 = 0.6$, and $f_3 = 0.3$ [14]. This is correct for completely random diffusion processes in the liquid. Using the high temperature approximation gives

$$\frac{N_+}{N_-} = 2(|\mu_n| + 1/2 \frac{S}{S+1}|\mu_e|)H_0/kT .$$

For this case the enhancement becomes

$$\varepsilon = (1 + 1/2 \frac{S}{S+1} \frac{|\mu_e|}{|\mu_n|}) .$$

The maximum enhancement occurs for complete saturation, i.e.

$$\frac{|\mu_e|}{|\mu_n|} = 657 .$$

Therefore,

$$\varepsilon_{max} = 323.5 .$$

To display the enhancement as a function of saturation, define the

saturation parameter:

$$S' = \frac{s}{s \ 1} \ .$$

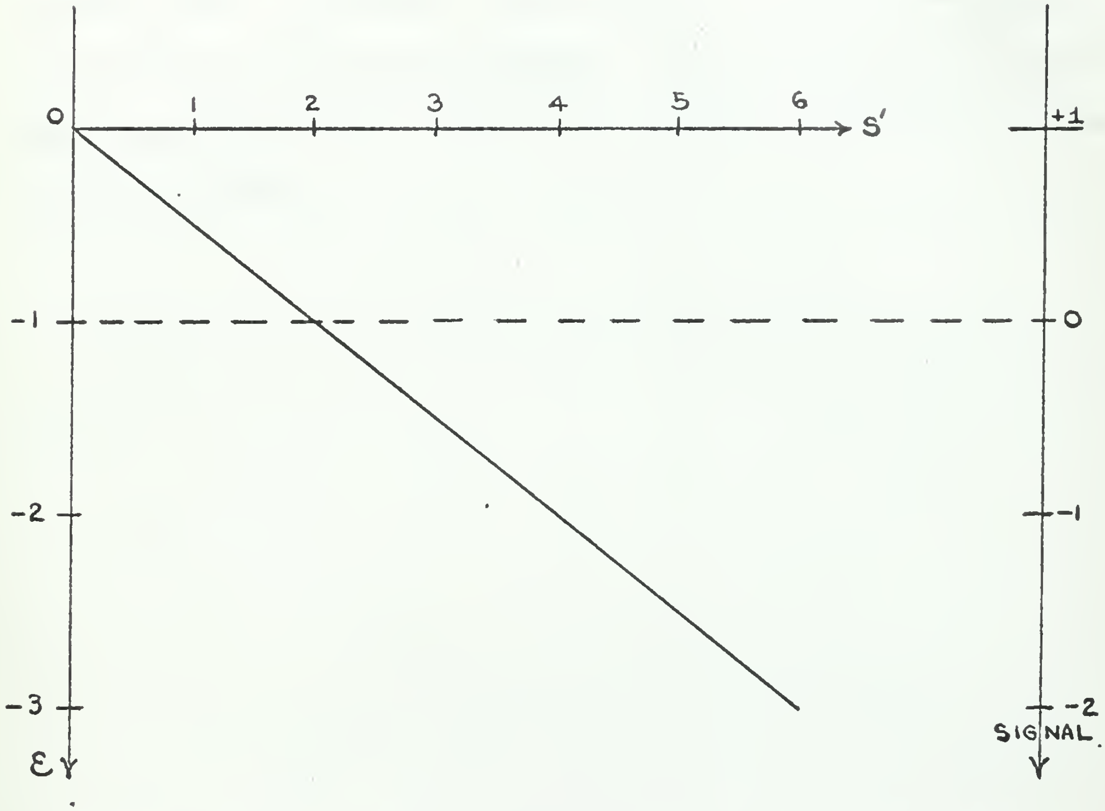

Plot of Enhancement and Signal vs. the Saturation Factor

Figure 3.

"Signal" as used in Fig. 3 is that signal which would be observed in a modulated field nuclear resonance experiment. (See Appendix A.). Positive signal represents absorption of energy while negative signal represents energy provided by the spin system to the nuclear resonance apparatus. This negative absorption may be utilized in a maser oscillator as described in Section 7.

Difficulties in the measurement of magnetic fields by utilizing dynamic polarization are encountered which have not been treated in the

foregoing analyses. The first is the shielding effects of paramagnetic and diamagnetic centers in the sample material. That is the impurities in the sample tend to insulate the nuclear spins from the external field. The second is frequency shift encountered at resonance. The frequency shift caused by the absorption is zero at resonance but is non-zero on either side of resonance. This frequency shift makes the tuning of the electronic circuits more difficult. These problems are of relatively minor significance to the experimental equipment used and will not be considered further.

6. The Maser Oscillator.

It has been shown that for sufficient saturation of the electronic resonance line the nuclear spins may be made to give up energy to an electric circuit. This property suggested to various observers the use of dynamic polarization in a molecular amplifier [8] or in a maser oscillator [14] . The theory for the nuclear maser oscillator has been developed by the group under Abragam at the Centre d'Etudes Nucleaires, Saclay, France and has been published in part in [10] , [12] and [14] . The following arguments are taken from these basic references.

A diagramatical realization of the maser oscillator is shown in Fig. 4.

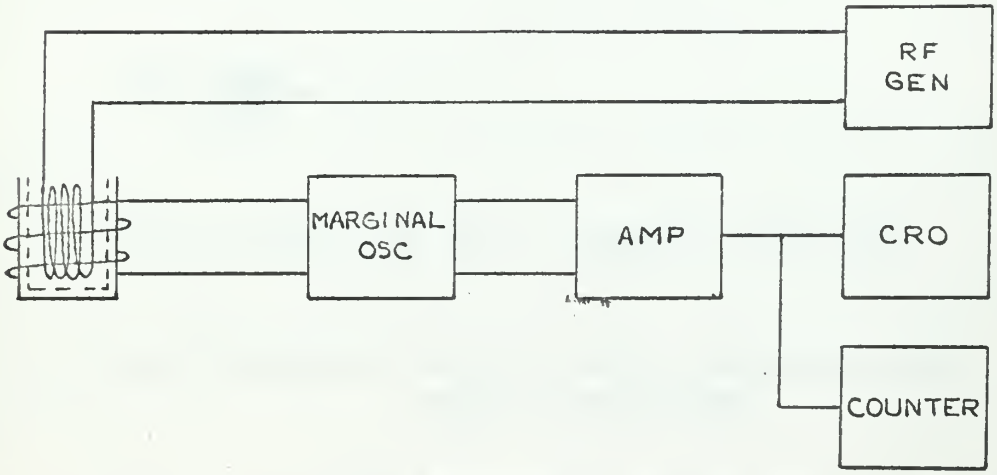

Maser Oscillator Block Diagram

Figure 4.

The electronic performance of the circuit may be described in terms of quality factors for the sample/coil circuit.

$$Q = 2\pi \frac{\text{energy stored}}{\text{energy dissipated per cycle}} \qquad (1)$$

$$Q_{\text{Loaded}} = \frac{\text{total stored Energy}}{\text{Output Energy dissipated in the resonator}}$$

One may write

$$\frac{1}{Q_s} = \frac{\text{Output Energy}}{\text{Total stored energy}} - \frac{\text{Energy dissipated in resonator}}{\text{Total stored energy}} \qquad (2)$$

where:

$$Q_s \overset{\text{D}}{=} \frac{\text{Total stored Energy}}{\text{Energy coupled in by Spin Coupling}} \quad .$$

Also let $Q_u \overset{\text{D}}{=} \text{unloaded } Q = \dfrac{\text{total stored Energy}}{\text{Energy dissipated in the resonator}}$.

Therefore from (2) and noting that Q_s refers to energy added to the circuit and is of sign opposite to the other Q's:

$$\frac{1}{Q_L} = \frac{1}{Q_u} - \frac{1}{Q_s}$$

or

$$Q_L = \frac{Q_u Q_s}{Q_s - Q_u} \quad . \qquad (3)$$

For

$Q_L > 0$, and $Q_u < Q_s$, Q_L is maximized if $Q_u \approx Q_s$.

For

$Q_u = Q_s \Rightarrow Q_L = \infty$ and this is the condition for the start of oscillation.

For

$Q_u \geq Q_s \Rightarrow Q_L < 0$, more energy is being added than dissipated and sustained oscillations may exist.

Realizable coils have unloaded Q's much less than that required for the maser oscillator. A marginal oscillator of the appropriate frequency may be added to couple sufficient energy to the detection

coil so that the effective Q_u is that required above.

This simple approach might be applied to any form of oscillator, however adequate treatment must include the nuclear effects upon which the device depends. The conditions for oscillation of the nuclear oscillator may be calculated from first principles for all levels of oscillation and not from just the conditions to start oscillation as is the case in the usual electronic oscillator.

Nuclear spins in a liquid can be accurately described by the phenomenological equations of Bloch [14]. Solving these differential equations gives the transient and steady state behavior of the system. The start oscillation condition becomes [14]

$$Q_U = (-2\pi\eta T_2 M_0)^{-1}$$

where:

η = filling factor

T_2 = transverse relaxation time

M_0 = d.c. magnetic moment of nuclei in the sample

The use of an electronic circuit whose frequency may vary from the precise value required by the nuclear resonance makes possible a study of the effect on maser oscillation with variation of the frequency, ω_c, of the tuned detection coils and marginal oscillator. The relation is

$$\frac{\omega_c - \omega_0}{\omega_c} \leq \frac{1}{2}\sqrt{\left(\frac{1}{Q_S} - \frac{1}{Q_L}\right)\frac{1}{Q_L}}$$

This value is maximized when $Q_L = 2Q_s$ whence

$$\frac{\omega_c - \omega_0}{\omega_c}_{MAX} = \frac{1}{4Q_S}$$

The value thus obtained may be converted to frequency and thence to field by using the simple relations of Section 2. For a Q_s of 300 the oscillator will continue to oscillate for a frequency range corresponding to a field variation of $\pm 40\Gamma$ ($1\Gamma = 10^{-5}$ oersted).

Assuming maximum bandwidth is chosen for the oscillation condition the effect of frequency pulling must be determined. This is given by [10]

$$\omega - \omega_0 = \frac{\Delta\omega_0}{\Delta\omega_0 + \Delta\omega_c}(\omega_c - \omega_0) ,$$

where

$$\Delta\omega_0 = \frac{\text{the proton line width}}{2} \quad \text{and}$$

$$\Delta\omega_c = \frac{\text{circuit resonance width}}{2} .$$

Using the same Q_s as before it is found that the measured field varies at most by 2.5Γ from the exact field value. This is no limitation on the inherent system accuracy which may be obtained by sacrificing bandwidth to gain sensitivity. Furthermore, since the circuit constants are known, exact frequency may be calculated using the relation above by the simple expedient of measuring the frequency of oscillation, ω_c, in the absence of Overhauser Effect.

If one corrects the frequency pulling, the inherent accuracy of field measurement depends only on noise. For amplitude noise alone,

$$\Delta_1\omega = \frac{1}{\rho_1\tau}$$

where:

$\Delta_1\omega$ = frequency error due to amplitude noise,

ρ_1 = signal to noise ratio, and

τ = measurement interval.

For phase noise the result is

$$\Delta_2\omega = \frac{1}{\rho}\sqrt{\frac{\omega}{Q_L\tau}}$$

where:

$\Delta_2\omega =$ frequency error due to phase noise.

Freycenon and Solomon [10] have calculated noise for the example $Q_S = 300$ and find that if $\tau > 0.1$ and $\rho/\rho_1 = 5$, only the amplitude noise is significant.

7. The Experimental System.

The inherently slow data rate of a free precession magnetometer underlies the reasons for the studies made in connection with this thesis. Initially the study was pointed broadly toward methods for increasing the data rate. A two pronged attack was begun. The first was in studying a fast pulse free precession magnetometer, that is one where continuous nuclear spin resonance is attained by an initial DC polarization followed by appropriately timed very short polarizing pulses which would keep the spins processing at some average value, allowing continuous determination of the nuclear resonant frequency. The second approach was to study the application of the Overhauser Effect to magnetometers and specifically to find a material of long lifetime suitable for a practical magnetometer. The latter was investigated in this study.

In an experimental study of the Overhauser Effect for application in an earth's field magnetometer one must be able to produce the effect in the earth's field in a manner akin to that to be used in a practical magnetometer. Three experimental techniques meeting this requirement were considered:

(1) Modulated Field Absorption

(2) Maser Oscillator Magnetometer

(3) Modified Free Precession Magnetometer

The Modulated Field technique, discussed in Appendix A, is not as readily applicable to magnetometers and was included primarily as an alternate approach in case the remaining two could not be achieved. A maser oscillator based on that described in [10] and a modified free precession magnetometer similar to that of Cooper [9] were constructed. These two experimental setups are described in general terms in subsections a and b which follow. The remaining subsections detail the

major components of the systems and the more important design considerations.

a. The Modified Free Precession Magnetometer.

This is basically a modified version of the standard Varian free precession magnetometer. The modifications consist of the addition of an r.f. generator, a magnetometer head containing an r.f. polarizing coil and a much smaller DC power supply which replaces the regular power supply. The remainder of the magnetometer, the preamplifier, amplifier and switching circuits, remain unchanged with the exception that provision is made to pulse the r.f. generator as well as the DC power supply. Block diagrams of the unmodified and modified systems are shown in Figs. 5 and 6.

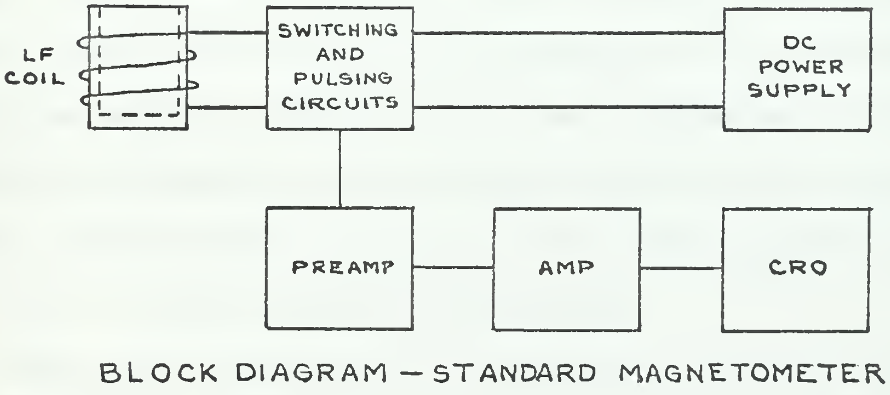
LF COIL
SWITCHING AND PULSING CIRCUITS
DC POWER SUPPLY
PREAMP
AMP
CRO
BLOCK DIAGRAM — STANDARD MAGNETOMETER

Figure 5.

The operation of the equipment is as follows. Pulses of r.f. power and DC current are supplied simultaneously to the r.f. polarizing coil and to the sample - detection coil. The r.f. power causes the electron resonance in the sample solution to become saturated, inducing the Overhauser Effect. The DC current is used to provide phase coherence to the precessing protons in the sample. The currents are cut off and the

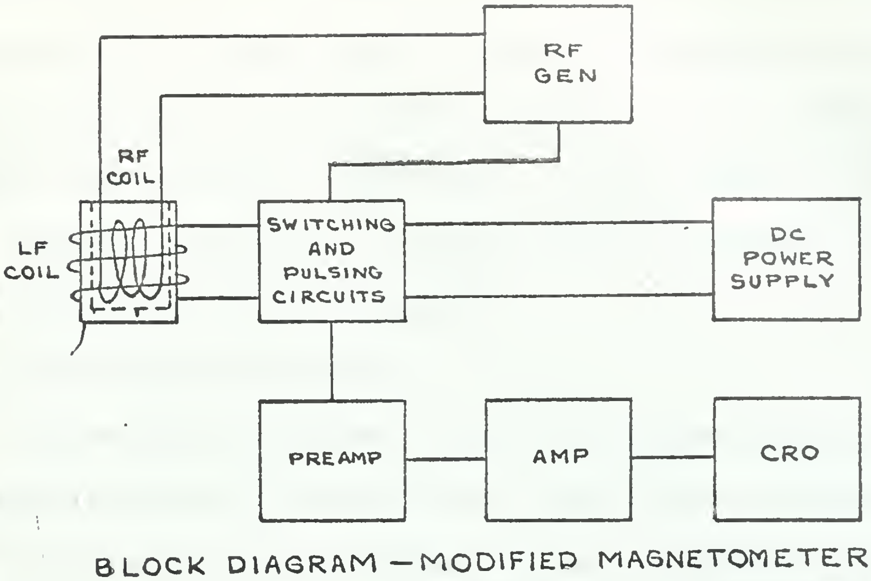
RF GEN
RF COIL
LF COIL
SWITCHING AND PULSING CIRCUITS
DC POWER SUPPLY
PREAMP
AMP
CRO
BLOCK DIAGRAM — MODIFIED MAGNETOMETER

Figure 6.

magnetic moment vector of the proton is allowed to precess about the earth's field vector, inducing a small voltage in the receiving coil. This voltage is then amplified and displayed on an oscilloscope. Since the purpose of this experiment was to demonstrate the Overhauser Effect, no attempt was made to further instrument the equipment so as to measure very accurately the value of the earth's magnetic field.

b. The Maser Oscillator Magnetometer.

This setup utilizes the r.f. generator and magnetometer head used in the previous setup plus a marginal oscillator and amplifier. A block diagram of the equipment layout is shown in Fig. 4.

The equipment operation is as follows. The r.f. generator provides continuous power to the r.f. coil, dynamically polarizing the protons of the sample. The energy coupled by the nuclear spins to the detection coil causes the marginal oscillator to oscillate at the precession frequency of the protons. Thus, by measuring the frequency of the marginal oscillator one may determine the value of the earth's field.

In order to insure that the frequency of the marginal oscillator is near that of the precessing protons, the oscillator frequency may be adjusted prior to operation by observing the Lissajous pattern produced by the frequency of the marginal oscillator and the signal obtained from a free precession magnetometer. In this manner the frequency of the marginal oscillator is adjusted until it corresponds very closely to the frequency of nuclear resonance.

c. Marginal Oscillator.

The marginal oscillator is used in the maser circuit to provide positive feedback to the sample coil tank circuit, artificially increasing the circuit Q and satisfying the maser conditions of Section 6. During maser oscillation the oscillator frequency depends on the external magnetic field through the nuclear resonance condition. The magnetic field is determined by the measurement of the oscillator frequency.

The requirements on the oscillator in terms of temperature and frequency stability are great. The gain of the oscillator must be conveniently adjustable so that the Barkhausen condition, $A\beta = 1$, may just be met. Noise performance of the oscillator must be quite good since the signal levels are low and any noise introduced will have an adverse effect on the accuracy of magnetic field measurement.

The oscillator may be considered as a servo system. In this regard the damping in the marginal condition must be small enough so that field changes may be followed rapidly but sufficiently great so that the oscillator will not "run away" into self-sustained oscillation either in the presence of noise or the nuclear signal. The oscillator must thus "lock" on the nuclear signal.

The oscillator circuit must work in a region of high noise. This noise consists primarily of power line harmonics coupled in from the

r.f. circuit. Normally the presence of high order powerline harmonics from power supply ripple in the r.f. oscillator does not cause any difficulty when working at moderate voltage levels. In the marginal oscillator, however, the expected signal and the power line harmonics have approximately the same amplitude, resulting in noisy operation.

Several marginal oscillators were constructed before one was found that would meet the requirements. A brief account of the various oscillators and their characteristics follows.

The first marginal oscillator was adapted from the simple circuit of [11] as shown in Fig. 7.

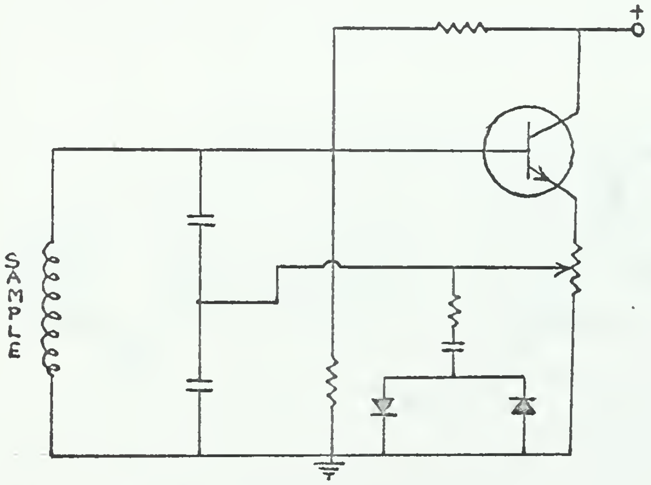

Simplest Marginal Oscillator

Figure 7.

At frequencies much higher than the desired 2KCS this oscillator was quite tractable and stable. At 2 KCS, however, oscillation became more difficult to obtain and the damping was much greater. The level of oscillation was seriously affected by temperature.

In view of the stability problems encountered with the oscillator of Fig. 7, a phase shift oscillator was constructed. To provide the necessary stable gain a broad band general purpose laboratory amplifier

was chosen. Such commercial amplifiers are readily available with gains adequate for suitable performance (20-40db). Using a simple r-c network as the adjustable phase shift element the circuit (Fig. 8) was found to have excellent marginal oscillation properties at 2 KCS. Various ambient harmonics of 60 cps such as the 35th and 36th, were readily detected by beating with the oscillator frequency. Noise performance was poor. The circuit was adversely affected by r.f. and 60 cps noise. A simple LC filter eliminated the r.f. problem but filtering the low frequency interference proved more difficult and the added circuit complexity made the oscillator undesirable.

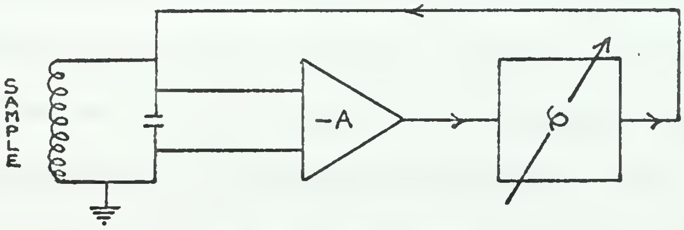

Phase-Shift Oscillator

Figure 8.

In order to use the high gain, temperature stable characteristics of the preceeding device and eliminate the noise problems, a band pass transistor amplifier was constructed. This consisted of a pair of complementary transistor amplifiers separated by a very high Q resonant circuit. Variable feedback and AGC elements were included to improve performance at very low levels of oscillation. This oscillator, while presenting no theoretical deficiencies, was found to be quite difficult to control at low levels, and was converted to a narrow band amplifier

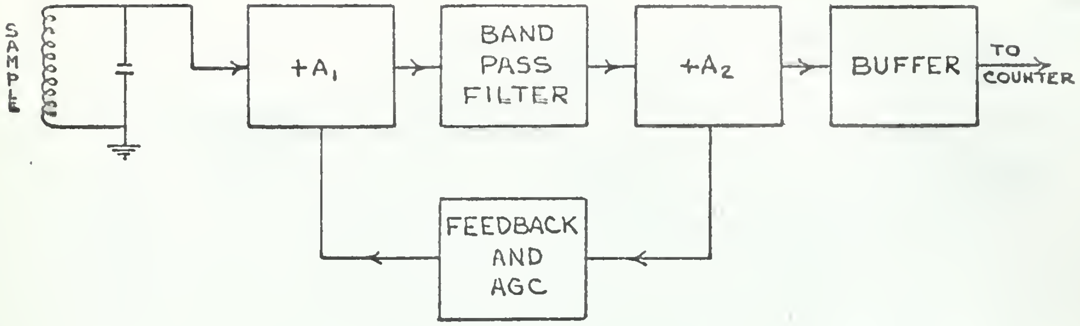

Band Pass Amplifier/Oscillator

Figure 9.

for use with subsequent oscillators.

In the literature a quite common vacuum tube marginal oscillator circuit is made from a cathode coupled amplifier as described in [10] . A transistor version of this circuit was constructed. Very careful attention was paid to r.f. bypassing to eliminate some of the noise problems previously encountered. Performance was good except for the temperature stability which was poor. It was both easier and cheaper to convert to a vacuum tube circuit rather than attempt to stabilize the transistorized version.

The oscillator of Fig. 10 exhibits stable characteristics in the vicinity of resonance. The effect of powerline harmonics are of little significance. Careful bypassing, including a capacitor placed directly on the input grid, was effective in reducing r.f. effects. The gain of the oscillator was variable over a wide range with the resistor, R. Frequency tuning over a few cycles per second was given by a small variable capacitor in parallel with fixed capacitors which are the correct value to tune the coils approximately to resonance.

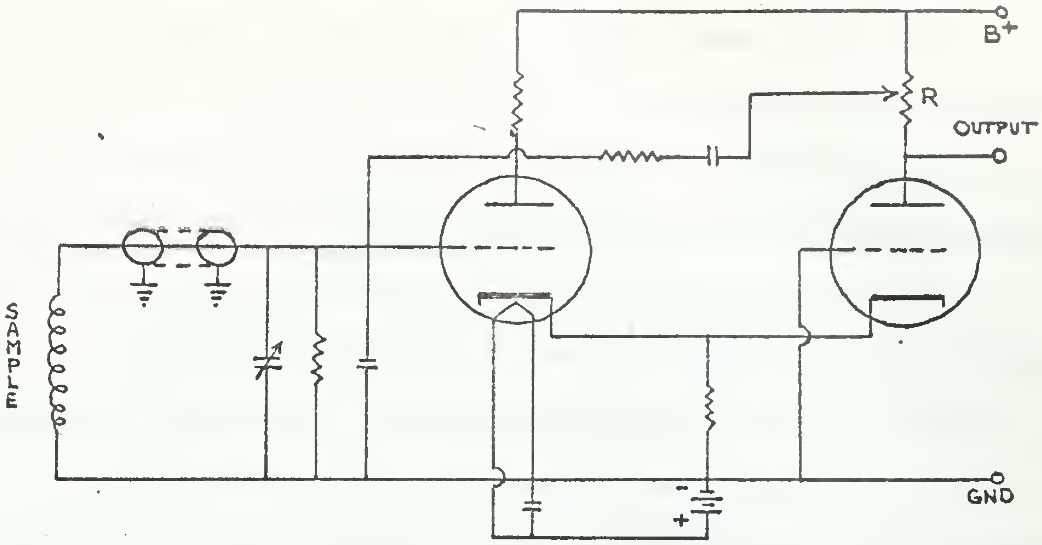

Marginal Oscillator in Final Form

Figure 10.

d. Sample-Detection Coil.

The sample coil serves a two-fold purpose, acting both as a coupling element between the nuclear spins and the electronic circuit and as a frequency determining element for the electronic oscillator. The various functions impose conflicting requirements which must be balanced in determining a final coil design.

In the electronic oscillator, the sample coil is an element of a parallel resonant circuit whose resonant frequency is about 2 KCS. The discussion in Section 6 shows that the unloaded coil Q should be high in order that the required positive feedback from the oscillator circuit be held to a minimum. A high Q circuit operating at 2 KCS requires a large value of inductance. A simple calculation shows that for an inductance in the millihenry range, a resonating capacitance of the order of a microfarad is required.

The earth's field is by no means constant, varying not only diurnally but from location to location. To allow for this variation, the frequency of the resonant circuit must be variable over a few cycles per second.

The net nuclear polarization is dependent on the total number of nuclei in the sample and thus upon the sample volume. The signal depends also upon the effectiveness with which the coil volume is utilized. This is measured by the filling factor, η , which is defined as the ratio of the volume of sample material where the resonance phenomena occurs to the volume intersected by the alternating magnetic field created by the coil with which the resonance is observed. These volume requirements indicate that a large sample should be used in a large coil with a small number of turns of small diameter wire. But some compromise must be made to obtain a coil of many turns of large diameter wire required for high Q and ease of tunability.

The total sample size may not be increased indefinitely due to external field inhomogenities. An inhomogeneous field within the sample causes the protons in different portions of the sample to precess with different frequencies. The result is a decrease in the signal-to-noise ratio and a decreased output signal. In an extreme case, such as in a building containing a large amount of electrical equipment, the field gradients are high and no earth's field nuclear resonance may be observed. In open areas the gradients over volumes on the order of a liter are small. Gradients as large as 300 Γ per meter may be tolerable [10].

Another factor in field homogeneity is the material to be used in the coil and associated structure. This material must exhibit no magnetic properties, suggesting copper as a coil material. A good grade of copper containing few ferromagnetic impurities is required. Various cable connectors and other elements used in the vicinity of the coil must be investigated carefully for magnetic effects. As an example of a poor choice of material, rubber stoppers were tried in the sample containers. Investigation with a free precession magnetometer showed that

these stoppers created an order of magnitude loss in signal amplitude.

Two-coil arrangements are often used in free-precession magnetometers to provide noise reduction. These coils are connected in series so that noise signals appearing the same direction in both coils will produce no voltage at the output terminals. Nuclear signals will induce voltages of opposite polarity in each coil which add to give an output voltage. This is shown diagramatically below.

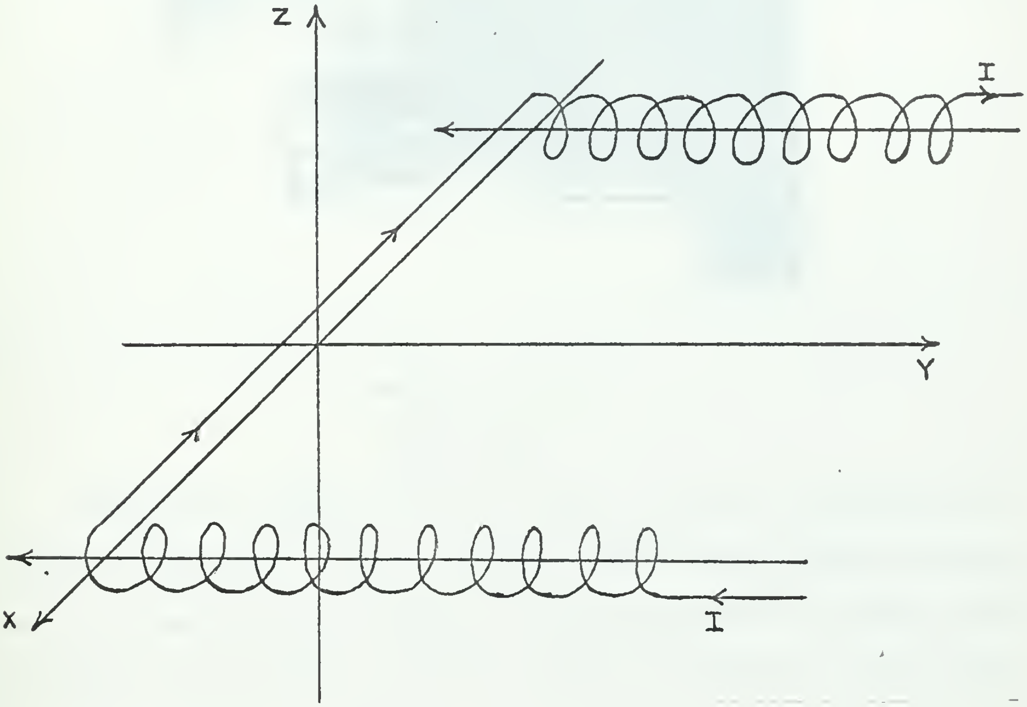

Dual Detection Coil Arrangement

Figure 11.

As a result of the foregoing a suitable coil may be chosen. For the investigations reported herein a double coil arrangement with an inductance of 23 mh was chosen. The coils each contained ten layers of 53 turns of AWG 15 enameled copper wire and had an inside diameter of two inches. Q measured at 1 KCS was 31. An additional factor in the choice of these coils was their suitability for use with a Varian free

precession magnetometer which was available and convenient for comparing operation with and without dynamic polarization.

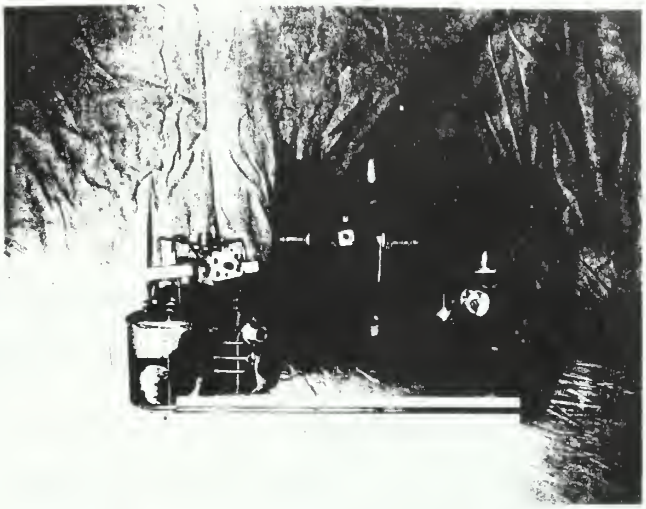

Detection Coils

Figure 12.

Another coil choice might be a single coil with an inductance of about 0.6 henry [10] . This inductance, while allowing smaller capacitance and somewhat easier tuning, is not applicable for use with a free precession magnetometer, due to the ringing encountered in pulsing the large inductance.

e. R. F. Enhancement Coils

The r.f. enhancement coils must be designed to provide a sufficient r.f. field in the sample to saturate the electron resonance. The specific criteria on this design are evolved from the saturation factor in Section 5 and from the sample size. Coils discussed here are paired to conform with the chosen two-coil detection coil arrangement.

From the sample size and shape the coil size and shape are developed. In general the r.f. coils should be as large as possible

and include as much volume of sample as possible. The r.f. coils must then conform closely to the inside dimensions of the sample container. The coil must have a high Q which dictates large wire and turns widely spaced to reduce distributed capacity. The high unloaded Q is necessary due to the large loading placed on the r.f. coils by the detection coil, sample, and marginal oscillator. This loading may be expected to reduce Q by one-half or more. The presence of the sample, a lossy dielectric placed within the coil, tends to create a distributed capacity and lower the self-resonant frequency of the coil.

Consider the equations which govern the saturation of the electronic resonance. Recall that

$$S = \gamma_e^2 H_1^2 T_1 T_2$$

The field in oersteds at the center of a coil of length, l, in meters, having N turns, for a current, I, in amperes is given by

$$H_1 = \frac{NI}{l} (4\pi \times 10^{-3}) \text{ OERSTED}$$

In this equation the length is fixed by the sample size and the current by the r.f. power source. The number of turns is the only parameter which may be easily varied to adjust the field strength, and thus obtain adequate saturation. For maser oscillation the saturation, s, must be greater than four and preferably greater than ten. The factors γ_e and the relaxation times are functions only of the material chosen. Thus for a given system the number of turns in the r.f. coils will determine the degree of enhancement. Note however, that increasing the number of turns lowers the self-resonant frequency and increases the inductance of the coil. The additional capacity encountered with the coils in the sample material may well be sufficient to make the coils

self-resonant below the desired operating frequency. This is undesirable in the sense that the tuning and matching are much more easily accomplished if the coils are self resonant above the desired frequency. As an example, a pair of two-turn r.f. coils connected in parallel in cylindrical samples two inches in diameter and four inches in length may be expected to have an inductance of about 0.2μh. For a current of 0.3 amperes in the coils and a sample with relaxation times $T_1 = T_2 = 10^{-6}$ sec. the saturation factor, s, may be computed to be much greater than ten as desired. The actual saturation attained was much less apparently due to high r.f. loss in the sample material.

f. R. F. Coil Matching.

In order that maximum r.f. power may be delivered to the sample, the r.f. coil impedance must be matched to that of the transmission line. The r.f. coil must have a length and diameter based on the chosen detection coil inside dimensions. Within these size considerations the effective saturation of the electronic resonance is increased by increasing the number of turns. The sample material acts as a lossy dielectric increasing the self capacitance of the r.f. coils. This lowers the self resonant frequency of the coils far below that normally expected for coils of the dimensions described above.

If the r.f. coils can be operated below self resonance then simple capacitive matching may be used.

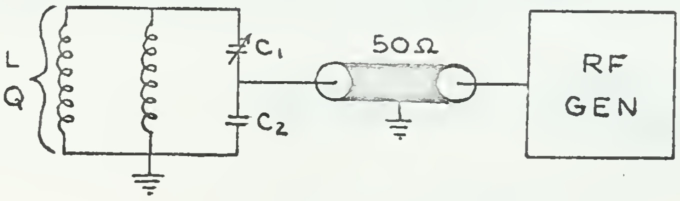

R. F. Coil Matching Network

Figure 13.

Here the series combination of C_1 and C_2 tunes L to resonance at the appropriate radio frequency. The capacitive divider C_1, C_2 is chosen so as to match the higher resonant impedance of the tank to the impedance of the transmission line. Solving for C_1 and C_2, for a coil with a Q greater than 10, gives:

$$C_2 = \frac{1}{\omega^2 L}\sqrt{\frac{Q X_L}{Z_o}} \qquad \text{and}$$

$$C_1 = \frac{1}{\omega^2 L\left(1-\sqrt{\frac{Z_{IN}}{Q X_L}}\right)} \quad .$$

As a practical matter the precise values of capacitance for C_1 and C_2 may not be met with standard capacitors. C_1 is the smaller of the two capacitors and is logically made variable.

The effect of the sample on the r.f. coils is such that the Q and inductance may not readily be computed and are best determined by measurement on an r.f. bridge. As a result of the measurement, values for C_1 and C_2 may be computed. C_1 is chosen variable over a small range including the computed value.

The match may be effected by bridge measurement. As C_1 is varied the impedance presented by the coil/matching network follows a circular locus as shown in Fig. 14. If the final experimental value of resistive impedance attained is other than that desired (A, in Fig. 14.), then the values of C_2 and C_1 are corrected using the following.

$$\frac{Z_{\text{IN DESIRED}}}{Z_{\text{IN EXPERIMENTAL}}} = \frac{\dfrac{Q X_L}{(1+C_2/C_1)^2}}{\dfrac{Q X_L}{\left(1+\dfrac{C_{2\,\text{EXP}}}{C_{1\,\text{EXP}}}\right)^2}}$$

$$R = \frac{C_2}{C_1} = \sqrt{\frac{Z_{\text{IN EXP}}}{Z_{\text{IN DES}}}}\left(\sqrt{\frac{Q X_L}{Z_o}}\right) - 1$$

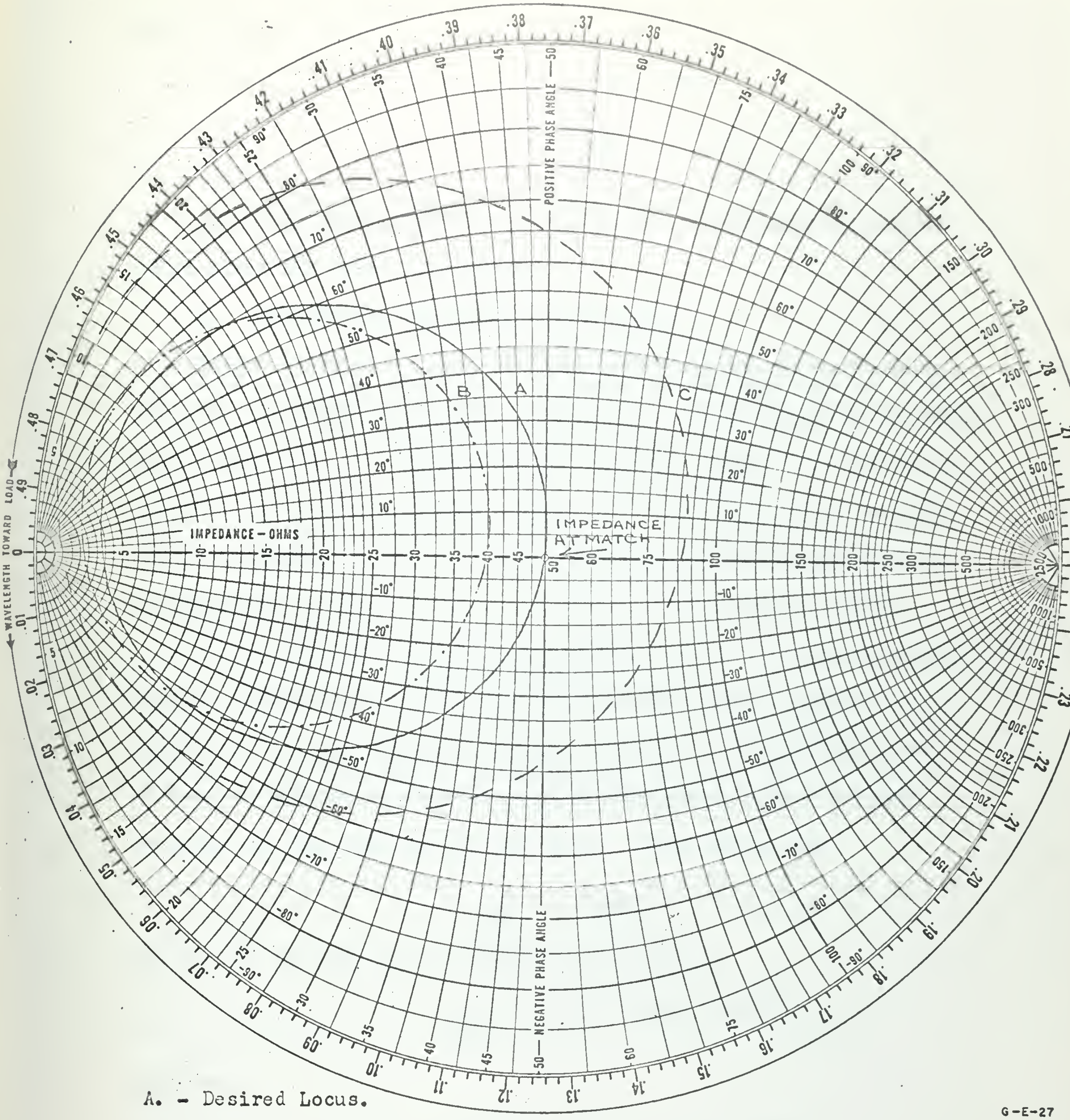

A. - Desired Locus.

G-E-27

B. - Resultant Impedance Less Than Required.

C. - Resultant Impedance Greater Than Required. $Z_o = 50\ \Omega$

Z-Θ CHART
MODEL 803A VHF BRIDGE
HEWLETT-PACKARD COMPANY
PALO ALTO, CALIFORNIA

Figure 14. Impedance Matching Loci

where finally

$$C_2 = \frac{1+R}{\omega^2 L} \quad \text{and}$$

$$C_1 = \frac{C_2}{R} \quad .$$

This simplified approach was found to give a reasonably accurate match after the first correction.

g. Determining the Saturation Factor.

Before attempting operation of the maser system one must ensure that the saturation condition is being met. A measurement of saturation may be made in a spectrometer but not with the sample and coil arrangements to be used in the maser system. Since the sample-coil arrangement is compatible with the modified free precession magnetometer, it is desirable to use this device to measure the saturation factor.

The modified free precession magnetometer may be operated without dynamic polarization as a normal free precession magnetometer. If a signal of equal amplitude is obtained from the same sample with and without an applied r.f. field, then the population ratios for the material are the same for the two cases. These ratios are

$$\frac{N+}{N-} = e^{\frac{2\mu_n H_1}{kT}}$$

for DC polarization and for dynamic polarization

$$\frac{N+}{N-} = e^{2\left[\mu_n + \frac{1}{2}\frac{S}{S+1}\mu_e\right] H_2/kT} \quad .$$

Equating:

$$e^{\frac{2\mu_n H_1}{kT}} = e^{2\left[\mu_n + \frac{1}{2}\frac{S}{S+1}\mu_e\right] H_2/kT}$$

or

$$\frac{S}{S+1} = \frac{2\mu_n (H_1 - H_2)}{\mu_e H_2} \quad .$$

H_1 is much greater than H_2, hence

$$\frac{s}{s+1} \approx \frac{2\mu_n}{\mu_e} \frac{H_1}{H_2}$$

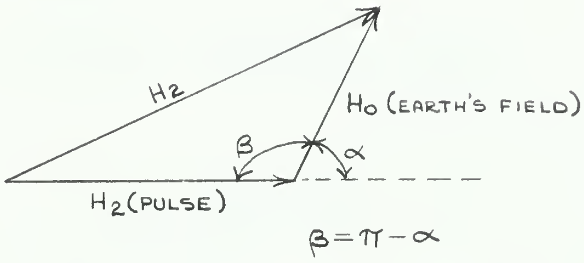

If it is assumed that $H_0 = 0.5$ oersted (earth's field), solving the vector diagram gives

$$\frac{s}{s+1} = \frac{3.03 \times 10^{-3} H_1}{H_2}$$

$$= \frac{3.03 \times 10^{-3} H_1}{\sqrt{H_2^2 - H_2 \cos\beta + 1/4}} \;.$$

For negative enhancement as required for maser operation, $s \geq 4$ or

$$\frac{s}{s+1} > 0.8 \,.$$

The field produced by the detection coil for a DC current is

$$H = 31\,I \,,$$

therefore

$$\frac{s}{s+1} = \frac{3.03 \times 10^{-3} I_1}{\sqrt{I_2^2 + \frac{I_2 \cos\beta}{31} + 2.6 \times 10^{-4}}} \;.$$

There is another means which can be used to check this result. If the DC current is varied while the r.f. frequency is held constant,

and the nuclear signal amplitude is recorded, the approximate electronic line width is traced out.

From the measured line width the electronic relaxation time, T_2, may be computed.

$$T_2 = \frac{1}{\gamma_e L}$$

where: L = Line width and

γ_e = electron gyromagnetic ratio.

Now recall

$$S = \gamma_e^2 H_1^2 T_1 T_2$$

As a first approximation, assume that $T_1 = T_2$, whence

$$S = \frac{H_1^2}{L^2}$$

h. Sample Materials.

Materials which exhibit Overhauser Effect range from the solids studied by Overhauser to the liquids and gasses studied by later investigators. In the magnetometer application liquid free radical solutions seem to offer the most promise.

A suitable material must have a long electronic relaxation time for ease of saturation as shown in Section 5. The electron spin-nuclear spin coupling should be strong to obtain large nuclear polarization.

The solvent for the free radical solution must contain a large number of nuclei (usually protons) to participate in the nuclear resonance. For measurement accuracy the nuclear resonance line width should be narrow and the nuclear relaxation time long. These conditions are met for dilute free radical solutions.

Free radical solutions are notoriously short lived. In a magnetometer the sample material must remain stable over a wide range of

temperature and other environmental conditions. Also the sample material should not deteriorate appreciably in the relatively long periods over which magnetic surveys are conducted. These times might range from a few hours to several weeks depending on the application. Free radicals are generally classed as stable or unstable. The unstable group have very short life and are not satisfactory for use in a magnetometer. Within the stable group lifetimes may vary from hours to several years. Short lifetime is due to chemical reactions taking place within the sample. Some specific reactions which contribute decomposition of the free radical are:

(1) reaction with itself

(2) reaction with oxygen

(3) reaction with solvent

(4) photolytic decomposition

(5) with, or in the presence of, the sample container.

Of these only the first is completely uncorrectible. The primary approach toward securing a slow decomposition rate is to remove very carefully any impurities, as for example oxygen, and to keep the sample cool. Specific procedures used with the various materials studied by these authors are discussed in Appendix C.

A listing of several free radical solutions with some important characteristics are given in table 1. A more detailed treatment on free radicals is given in [16].

To observe the Overhauser Effect the electron resonance line must be saturated. The particular frequency to use for best saturation in a particular field must be determined. The simplest means of determining the frequency is to find a reported electronic resonance experiment in the earth's field. Such reports were available only for peroxylamine

Table 1. Free Radicals

Material*	Electronic Resonance Frequency for H_o=1/2G.	Electronic Saturation	Preparation	Lifetime	Special Remarks
1	4MCS	easy	very difficult	long	tendency to burst container due to pressure
2	30-80 MCS	difficult	fairly easy	months	not very sensitive to air
3			involved but easy	months	extremely sensitive to air
4	50 MCS @H=17.8G	easy	involved but easy		very concentrated solutions required [14] very sensitive to air
5	55-56MCS	very easy	easy	500 hrs.	Very easy to use in magnetometer. rapid deterioration if heated, lifetime is pH sensitive, sulfamate ion may extend the lifetime of the material.

* The numbers listed under Material indicate the following:

1 - Na in NH_3

2 - α, α Diphenylpicrylhydrazil (DPPH)

3 - Benzophenone (Sodium Ketyl) in Tetrahydraforan

4 - Napthalene in 1,2 Dimethoxyethane

5 - $(SO_3)_2NO^{--}$, Peroxylamine disulfonate

disulfonate and Na in NH_3 for the materials listed in table 1.

To calculate the frequency of electron resonance in a material one might quite generally solve the Spin Hamiltonian for the material. A detailed knowledge as to the exact nature and structure of the material at some instant of time must be had for the solution. Needless to say, such calculations are exceedingly difficult.

Fortunately, a simpler method of solution exists where the nature of the material is fairly well known. That is, electron paramagnetic resonance experiments may be utilized to obtain an evaluation of the expected structure and to obtain the spin coupling constants, A, in gauss, and a g factor, ($g = 2.0023$ for electrons), for the material. With this information the Spin Hamiltonian may be solved. Fig. 15 shows the typical result of an electron resonance experiment.

There are limitations on the simplified calculations. The first limitation is that of the structure of the material. Since the calculation is quite complicated at best, the simplest structure which provides a reasonable fit is chosen. Transitions whose probability of occurrence are low are ignored at the outset. The second limitation is on the coupling constants. The measurement of the constants contains some known experimental error. Further, a single coupling constant is usually chosen to represent two or more spin couplings which are nearly, though not in general, equally spaced. Weak spin-spin coupling gives a resonance line broadening where the observed resonance lines are actually made up of many finer lines which are unresolved by the experimental equipment. Weak couplings and finite line width are largely ignored in the calculations.

The results of the calculations are surprisingly good in spite of the approximations. The free radical materials studied for this thesis

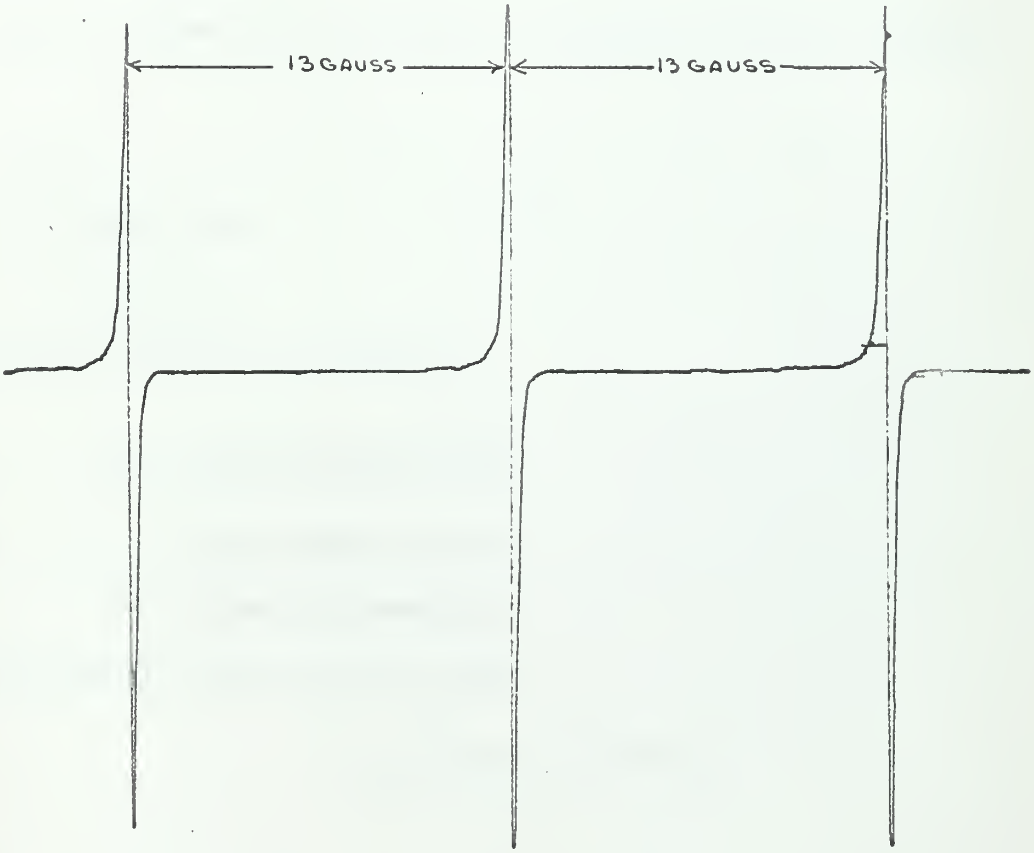

DERIVITIVE OF ELECTRONIC RESONANCE ABSORPTION
VS
MAGNETIC FIELD
FOR PEROXYLAMINE DISULFONATE
FIGURE 15

have been extensively studied and their characteristics are fairly well known.

To show the method of calculation consider a free radical solution having coupling between the electron and a single nucleus having a spin of one.

Let $\vec{I}$ = Nuclear Spin,

$\vec{S}$ = Electron Spin, and

$\vec{J}$ = Total Spin.

At equilibrium, in the absence of an external field, the spins are

$\vec{I} = 1$,

$\vec{S} = \pm 1/2$, and

$\vec{J} = 1/2,\ 3/2$.

The spin Hamiltonian $\mathcal{H}$ is given by

$$\mathcal{H} = g\beta \vec{H}\cdot\vec{S} + g\beta A \vec{I}\cdot\vec{S} ,$$

where β = Borh magneton and

A = Coupling constant.

Substituting the quantum numbers gives

$$E = g\beta\left[H_z S_z + A I_z S_z\right]$$

where $S_z = \pm 1/2$ and

$I_z = \pm 1, 0$.

For purposes of calculation the earth's field may be assumed negligibly small and a value of frequency for the zero field value only need be computed. The value thus obtained may be corrected by a small amount based on the slope of the curves of Fig. 18. The effective field at the nucleus may be expected to be >> the earth's field. There-

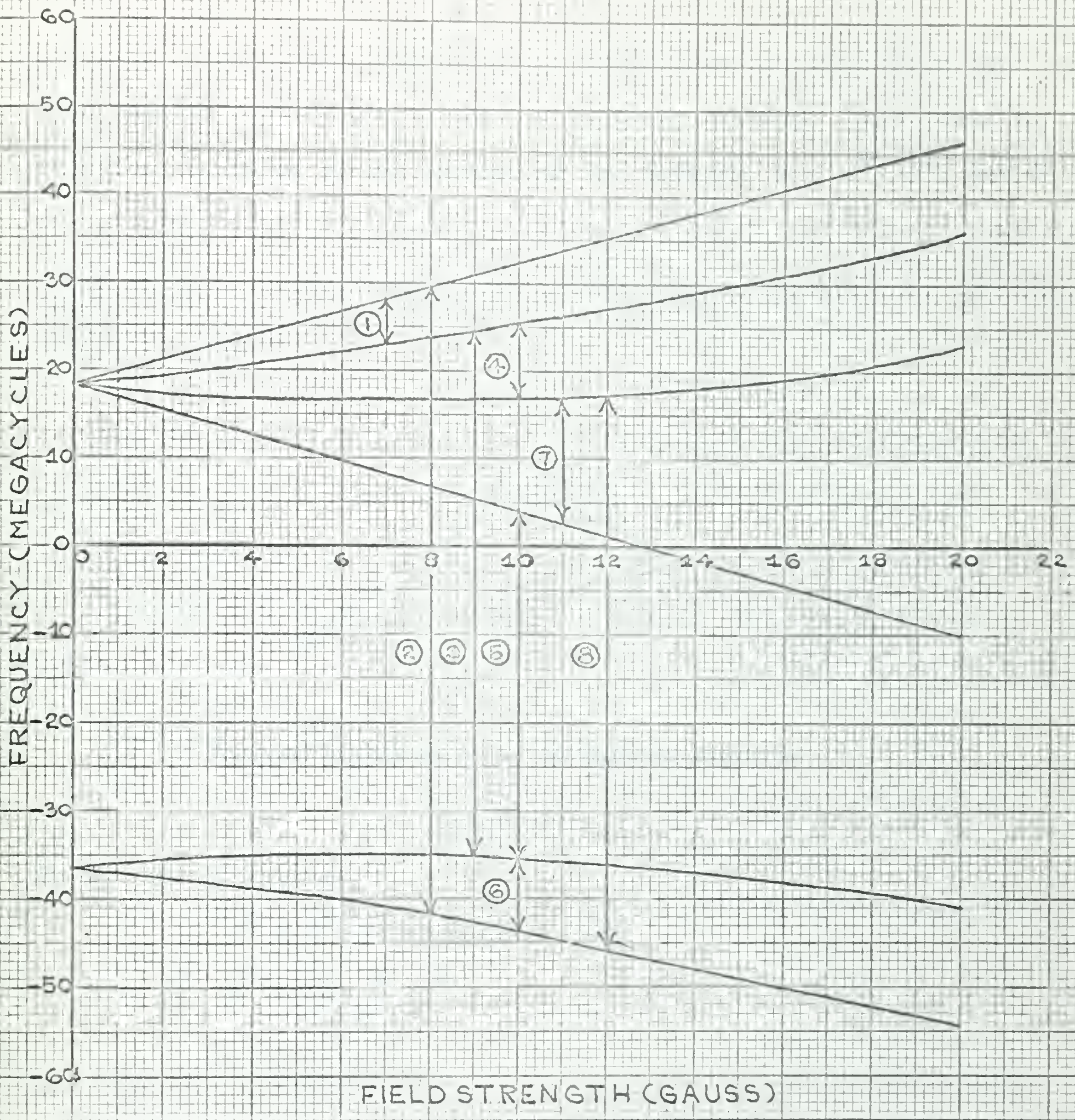

ZERO FIELD — f_0 = 54.731 MC f④ = 0.476 MC f⑧ = 54.748 MC
0.5085 GAUSS — f① = 0.468 MC f⑤ = 53.789 MC
f② = 55.692 MC f⑥ = 0.476 MC
f③ = 54.748 MC f⑦ = 0.484 MC

FIGURE 16
CALCULATED
LOW FIELD ENERGY LEVEL DIAGRAM
FOR
PEROXYLAMINE DISULFONATE MODEL

K&E 7½ X 10 INCHES MADE IN U.S.A.
KEUFFEL & ESSER CO.

fore

$$\mathcal{H} \approx g\beta A\, \vec{I} \cdot \vec{S} \ ,$$

In order to make this computation a vector model is used where the spin quantum numbers are treated as ordinary vectors. This leads to equations in terms of the squares of the vectors, i.e. J^2, I^2, and S^2. These values must be replaced by $J(J+1)$, $I(I+1)$, and $S(S+1)$ respectively since the actual magnitudes of the vectors are given as $\sqrt{J(J+1)}$, $\sqrt{I(I+1)}$, etc.

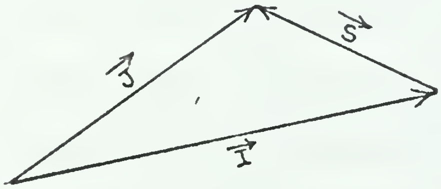

Vector Representation of Quantum Numbers

Figure 17.

By the law of cosines

$$J^2 = I^2 + S^2 - 2IS\cos\Theta \quad \text{and}$$

$$\vec{I} \cdot \vec{S} \quad \frac{J^2 - I^2 - S^2}{2} \ .$$

and this may be written as

$$E = g\beta A\left[\frac{J(J+1) - I(I+1) - S(S+1)}{2}\right] .$$

Further

$$\Delta E = 3/2\, g\beta A \quad \text{and}$$

$$\Delta \nu = \Delta E / h \ .$$

Now this result is applied to peroxylamine disulfonate where

$\Delta\nu$ is found to be approximately 54.7 MCS for $A = 13.0(\pm 0.05)$ gauss from Fig. 15. This is as far as hand calculation is practical.

A complete solution based on the same assumptions, that is $A = 13.0$ gauss, $g = 2.0054$, and single electron-nucleus coupling may be had by computer solution. A program to do this was obtained from Professor William Tolles of the U. S. Navy Postgraduate School. The results of the computation are shown in Figs. 16, 18, and 19. Fig. 16 is the energy level diagram plotted as frequency versus field intensity. This result is that obtained by the Breit-Rabbi formulas [1] .

Fig. 18 shows the electronic resonances which may be observed as a function of field. Note that in the earth's field (≈ 0.5 gauss) the frequencies are quite close to that predicted for zero field by the simple calculation previously described. With this picture the frequencies to be chosen for a particular pulse field of the free precession magnetometer may be determined.

Fig. 19 provides the final step in the analysis by providing a relative transition probability as a function of the field strength. The larger the transition probability (always ≤ 1) the more easily saturation is accomplished.

One might wonder at this point just how effective the calculations are. Muller and Haupt [15] studied peroxylamine disulfonate in a field of fifteen oersted. They measured the electronic resonance frequencies over a range of 20-80 MCS. Their experimental data with the computed data superimposed is shown in Fig. 20. The calculated amplitudes should be corrected for the fact that the higher the frequencies give more intense lines.

The second material studied was α , α , Diphenylpicrylhydrazyl,

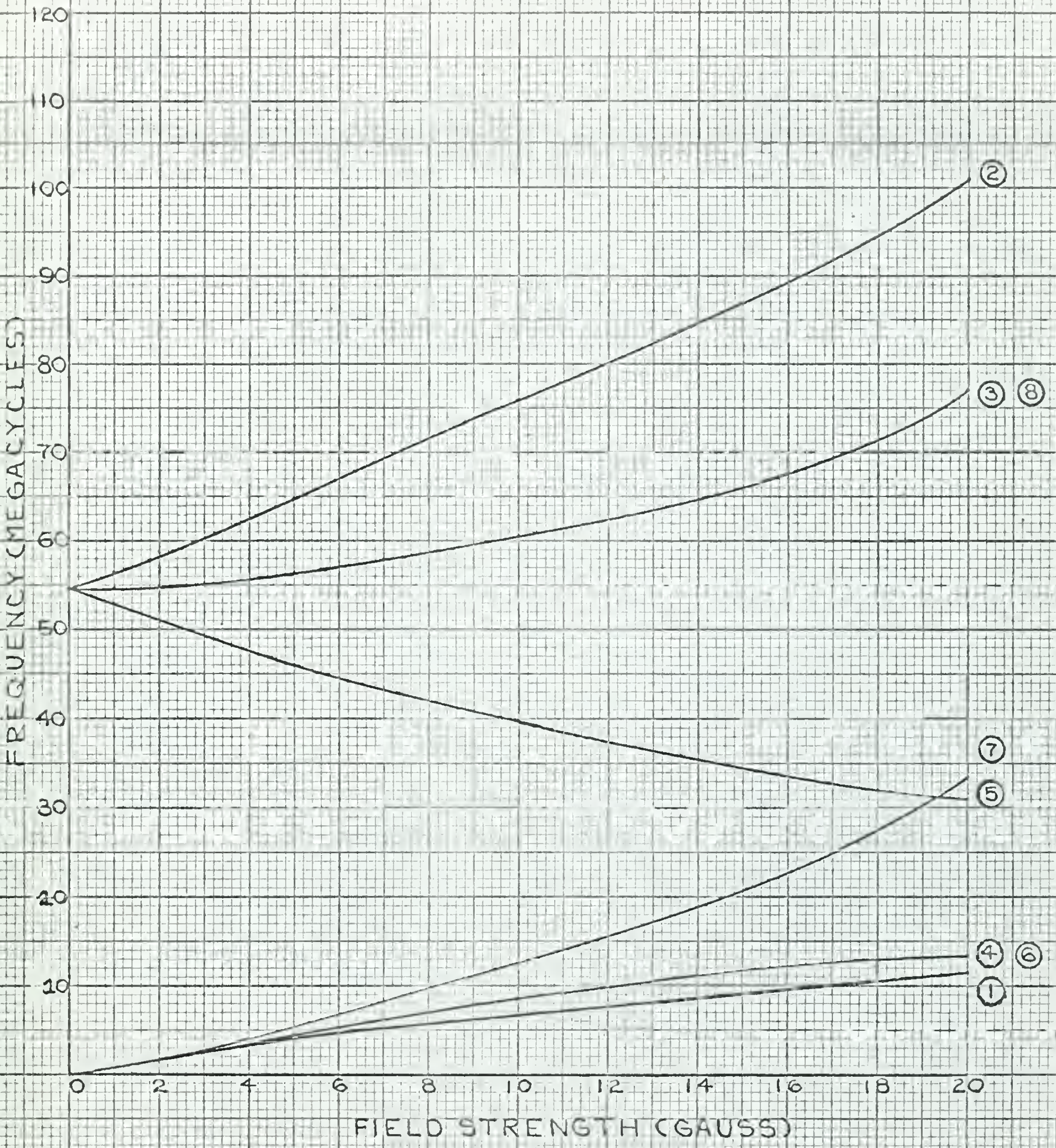

Figure 18
FREQUENCY VS FIELD STRENGTH
FOR ALLOWED TRANSITIONS IN
PEROXYLAMINE DISULFONATE MODEL

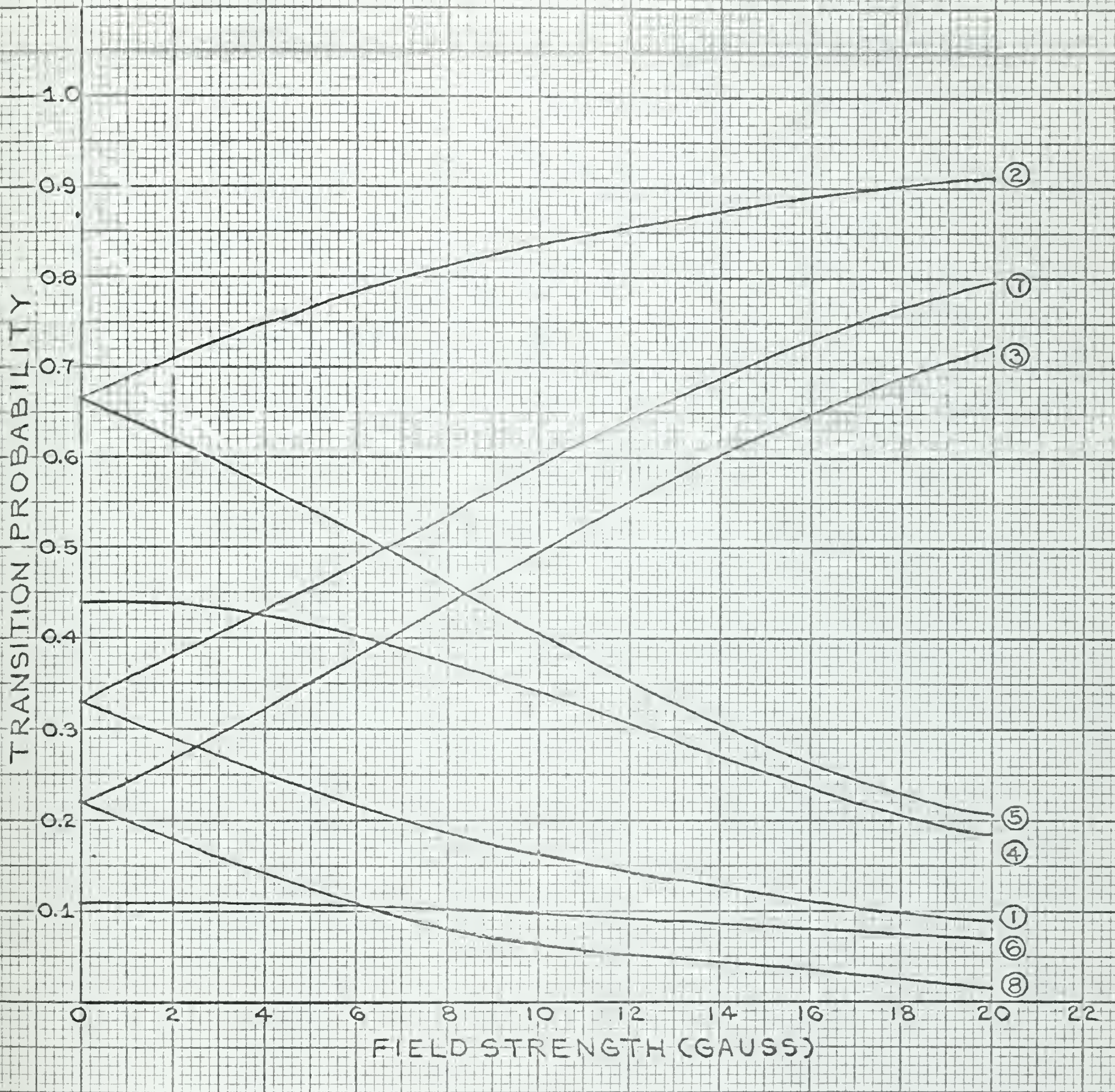

Figure 19
TRANSITION PROBABILITY VS FIELD STRENGTH
FOR
PEROXYLAMINE DISULFONATE MODEL

KEUFFEL & ESSER CO

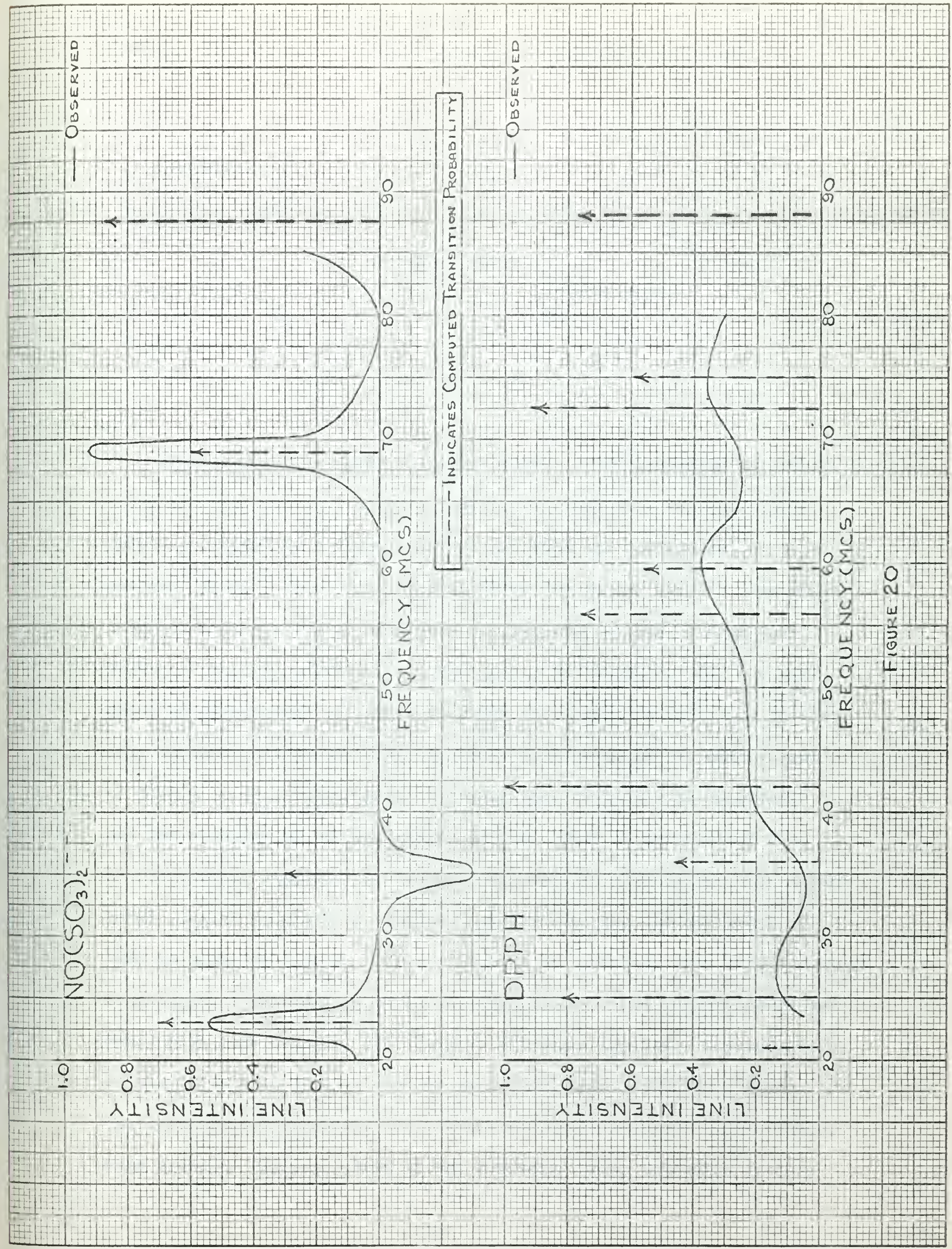

Figure 20

(DPPH). The structure of this material is generally shown as

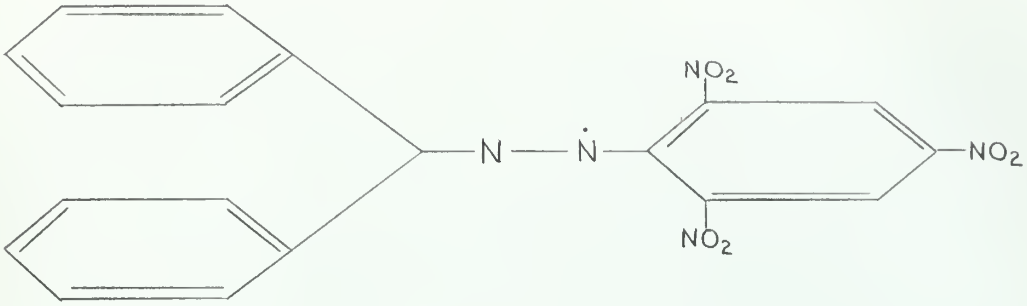

This material is found to give a fairly broad hyperfine structure. Again the material is a free radical in solution with benzene. The coupling assumed is between the free electron and two central nitrogen nuclei. It is further assumed that these two nuclei see the same adjacent structures which is obviously not the case as may be seen above. A single coupling constant, $A = 9.0$ gauss, is obtained. For the purposes of calculation all other coupling constants are ignored. To take into account each of the spin couplings would require the measurement of 30,375 lines at high field, assuming they could all be resolved, and the solution of the associated matrix. This is impractical even on the digital computer due to the very great solution time. The energy level diagram obtained by computer solution for the assumed model of DPPH is shown in Fig. 21. Note that with the addition of a single nuclear coupling over that for peroxylamine disulfonate, that the structure becomes much more complex. The complex structure implies a superposition of many resonance lines. For the more complicated structure, fewer (percentagewise) molecules may be expected to be involved in the resonance process. This is shown by the generally lower intensity factors

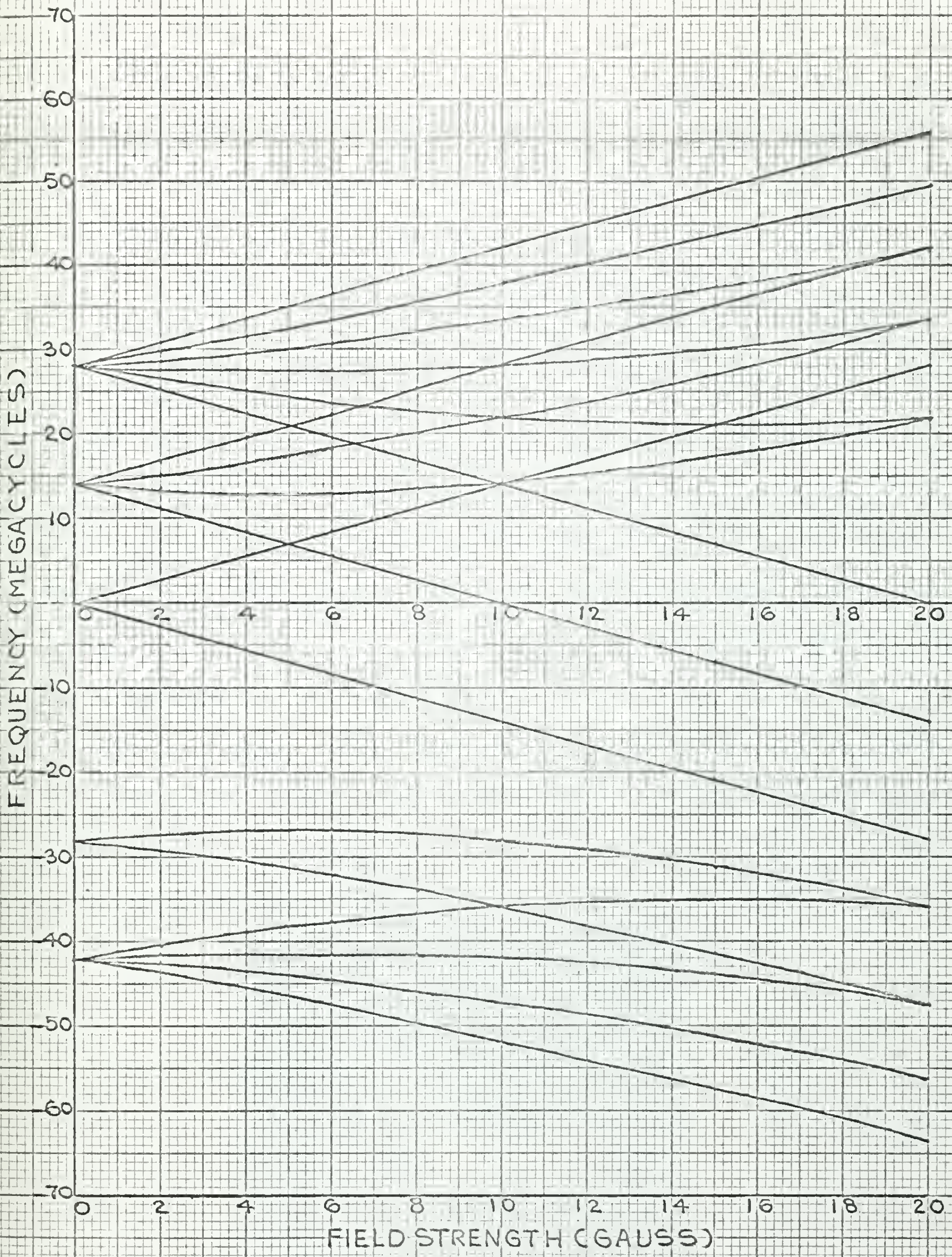

Figure 21
LOW FIELD ENERGY LEVEL DIAGRAM
FOR
DPPH MODEL

which are obtained for DPPH as compared to peroxylamine disulfonate. The calculated values are again compared with Muller and Haupt's values in Fig. 20.

8. Experimental Results.

The Overhauser Effect was observed using both the modified free precession magnetometer and the maser oscillator. The results obtained from the two experiments are given in the following sub-sections.

a. Modified Free-precession Magnetometer Experiment.

The modified free-precession magnetometer proved to be a very useful device for observing the Overhauser Effect. As is shown in Fig. 18, the electron resonance frequency varies with the value of the applied magnetic field. This experiment permitted one to adjust the applied field to suit a particular radio frequency. Thus, the Overhauser Effect may be observed over a range of several megacycles rather than at one critical frequency. This variation is very useful when attempting the experiment for the first time.

The procedure used to perform this experiment was to first apply the pulsed r.f. and DC fields to the sample. The DC field was then varied until a free precession signal was obtained. A typical free precession signal observed using this method is shown in Fig. 22.

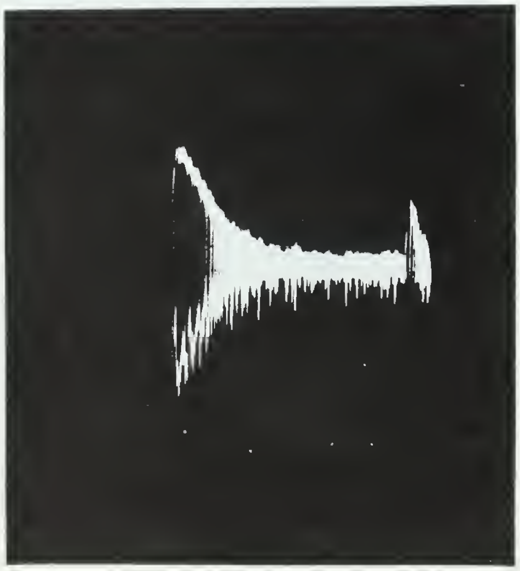

Scale:
0.2V/Cm Vertical
0.2 Sec/Cm Horiz.
fe = 57.5 MCS

Signal From Modified Free Precession Magnetometer

Figure 22.

Note that, in comparison to the signal shown in Fig. 1, the decay time of the signal is fairly short. Fig. 1 was obtained from a Varian magnetometer. The performance of the experimental coil was degraded by the rough handling to which it had been subjected and, very likely, by the presence of ferromagnetic impurities in the plastic containers which held the sample solution and the r.f. coils. Also, the coil was connected to a Varian preamplifier that contains tuning capacitors designed to resonate a Varian coil. The experimental coil was slightly off the preamplifier tuning range and was not precisely resonated. This also decreased the decay time.

To determine if the signal was, in fact, due to dynamic polarization and not due to DC polarization alone, the r.f. power applied to the sample and was varied from zero to its maximum value. With no r.f. power applied, no precession signal was observed. As the r.f. power was increased past the point of minimum electron resonance saturation, the signal amplitude increased.

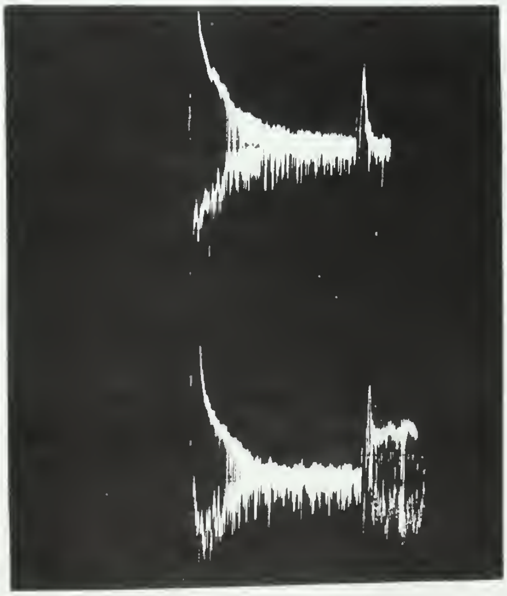

Scale:

.2V/Cm Vertical
.2 Sec/Cm Horiz.
2 amp DC Pulse

.2V/Cm Vertical
.2 Sec/Cm Horiz.
25 ma DC
fe = 57.5 MCS

Comparison of Normal and Dynamic Polarization

Figure 23.

To demonstrate the increase in signal amplitude that results from dynamic polarization, the r.f. field was removed. The DC polarizing current was then increased until a signal was obtained whose peak amplitude was equal to that of the signal observed with dynamic polarization. Fig. 23 shows the result of this test. To obtain the upper signal, a 2 ampere DC pulse was used to polarize the sample. The lower signal was obtained using a 25 milliampere DC pulse and dynamic polarization. The pulse duration was the same for both cases.

For given r.f. oscillator frequency and input power, the signal amplitude was observed to vary with the value of the applied DC polarizing field. Values of signal amplitude and DC polarizing current were recorded for two different values of electron resonance frequency. The results, which are, in effect, a tracing out of the electron resonance lines, are shown in Fig. 24. For a frequency of 55.5 MC, two peaks in signal amplitude, corresponding to the saturation of two electron resonance lines, were noted. The current pulse used to obtain the first resonance line represents the minimum current which may be used. From the field corresponding to this current, the saturation, s', is found to be greater than 0.8, the condition required for maser oscillation. Note that the value of field for the 57.5 MC frequency may not be used to calculate saturation, since the greater portion of the pulse merely serves to provide the ambient field required to give an electron resonance frequency equal to that of the r.f. oscillator. The broadening of the second resonance line is most probably due to inhomogeneities in the polarizing magnetic field. The positions of the peaks compare favorably with those predicted by Fig. 18.

Two, three, and four-turn r.f. coils were used in this experiment. The signal amplitude was smallest for the two-turn coil; largest for

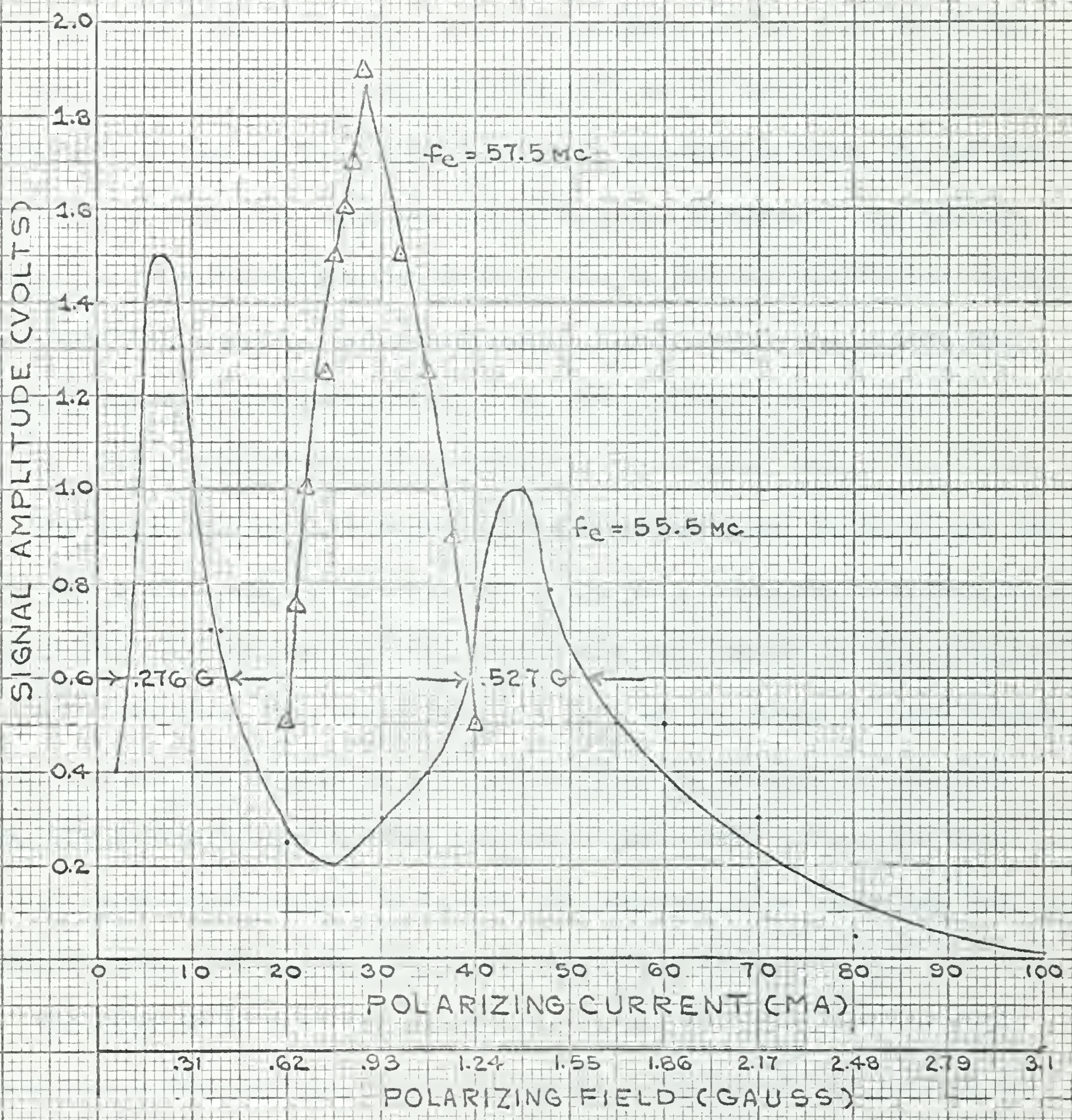

FIGURE 24

SIGNAL AMPLITUDE VS POLARIZING FIELD

FOR

PEROXYLAMINE DISULFONATE

the four-turn coil. The four-turn coil was used to obtain the results shown in Fig. 24.

The above results were obtained using a 0.01 molar solution of potassium peroxylamine disulfonate as the sample material. DPPH and benzophenone and sodium in tetrahydrofuran were tried using applied fields ranging from 0-20 gauss and frequencies ranging from 55-60 MCS. The Overhauser Effect was not observed with these materials. This is believed to be due to the short transverse relaxation time, T_2, of the materials so that only very low saturation was achieved. The failure to observe enhancement was not believed to be due to insufficient equipment sensitivity since, for peroxylamine disulfonate, the effect was observed for very low saturation, $S' < 1/4$. $(0 \leq S' \leq 1)$

b. The Maser Oscillator Experiment.

The procedure used to perform this experiment was to first set the frequency of the marginal oscillator using the technique described in Section 7b. The feedback in the system was then varied until, with no r.f. power applied, the oscillator was just on the verge of oscillation. The r.f. power was turned on and increased until oscillation started. Next, the feedback was adjusted to give a good level of oscillation. The r.f. power was reduced to nearly the minimum value necessary for sustained oscillation, to give increased sample lifetime.

The conclusion that the sinusoidal signal obtained was, in fact, due to maser oscillation and not due to self-sustained oscillation of the marginal oscillator, was based on the following observations.

(1) As the r.f. power was decreased, the level of oscillation decreased until, finally, oscillation ceased.

(2) As the radio frequency was varied above and below 55.5 MC, the level of oscillation decreased.

(3) As the frequency of the marginal oscillator was varied either side of the center frequency the level of oscillation decreased. If the oscillator frequency was varied far enough, oscillation ceased.

(4) A metallic object was placed in the vicinity of the sample coil. Due to the change in the field strength caused by its presence, the oscillator frequency was observed to change.

The signal obtained was fed to a period counter which gave a reading of signal period averaged over 10,000 periods. The output of the period counter was fed to a printer and to a chart recorder. A plot of the variation in signal period with time for approximately a one and one-half hour period is shown in Fig. 25. Full scale on the chart corresponds to 100 gamma. The dip in the curve at 1730 PST was caused by the presence of an automobile in the vicinity of the magnetometer coil. The spikes are caused by random digits generated in the counter.

The sample used in this experiment was, again, potassium peroxylamine disulfonate. The sample was used continuously for a period of some 16 hours with no noticeable decrease in signal amplitude. This represents a significant improvement over the two to three hour lifetime reported in [10] . Deterioration of the sample may be observed by loss of the light purple color present in a fresh solution. The sample used above showed only slight reduction in color after the 16 hours of use. Again, no results were obtained for the other two sample materials, DPPH and benzophenone and sodium in tetrahydrofuran.

The 4-turn r.f. coil was used in this experiment. It was not matched to the 50 ohm transmission line. Both the two and three-turn coils were tried but, the r.f. field produced by these coils was not sufficient to saturate the electron resonance adequately, although they were entirely satisfactory for use with the MFP magnetometer.

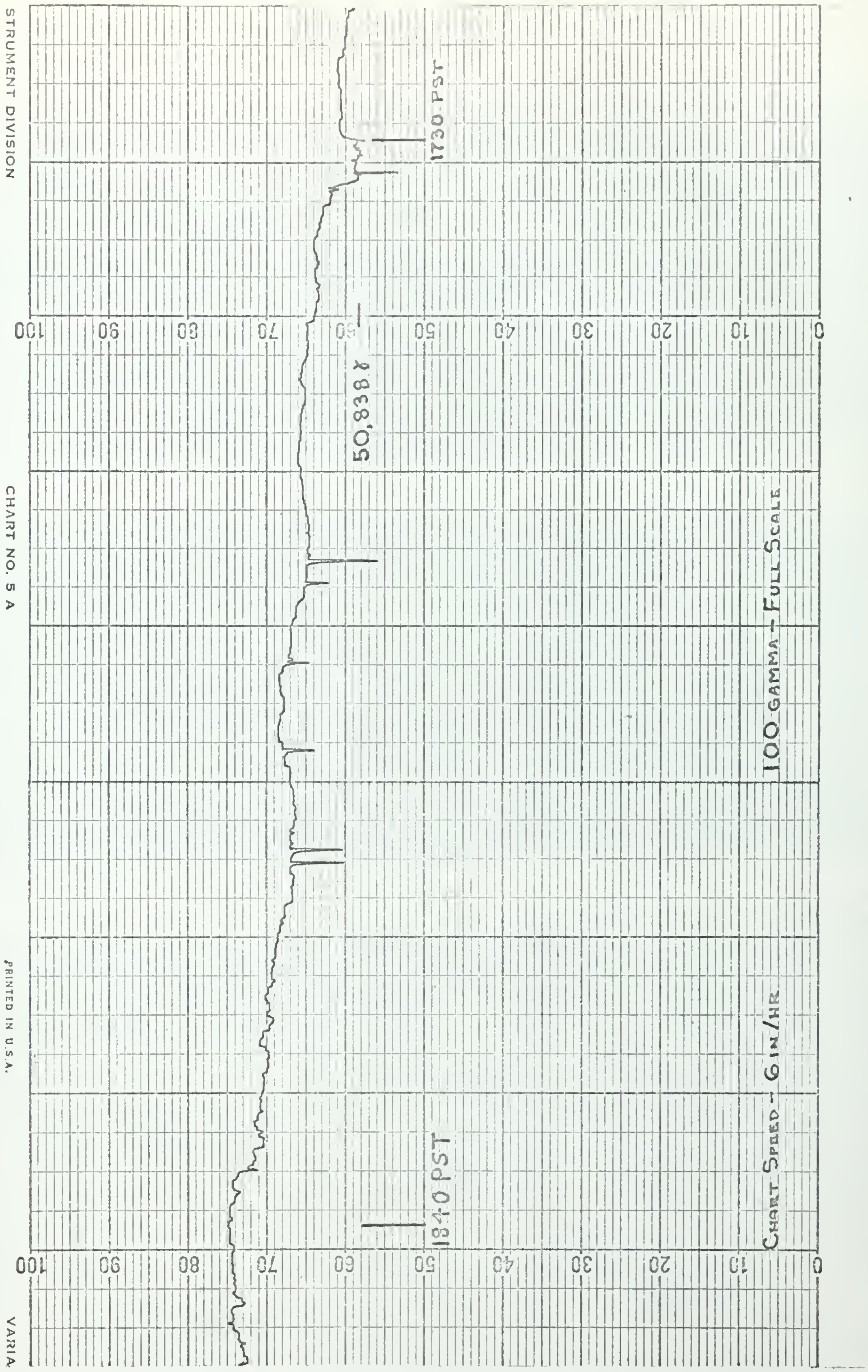

Variation of Signal Period with Time

Figure 25.

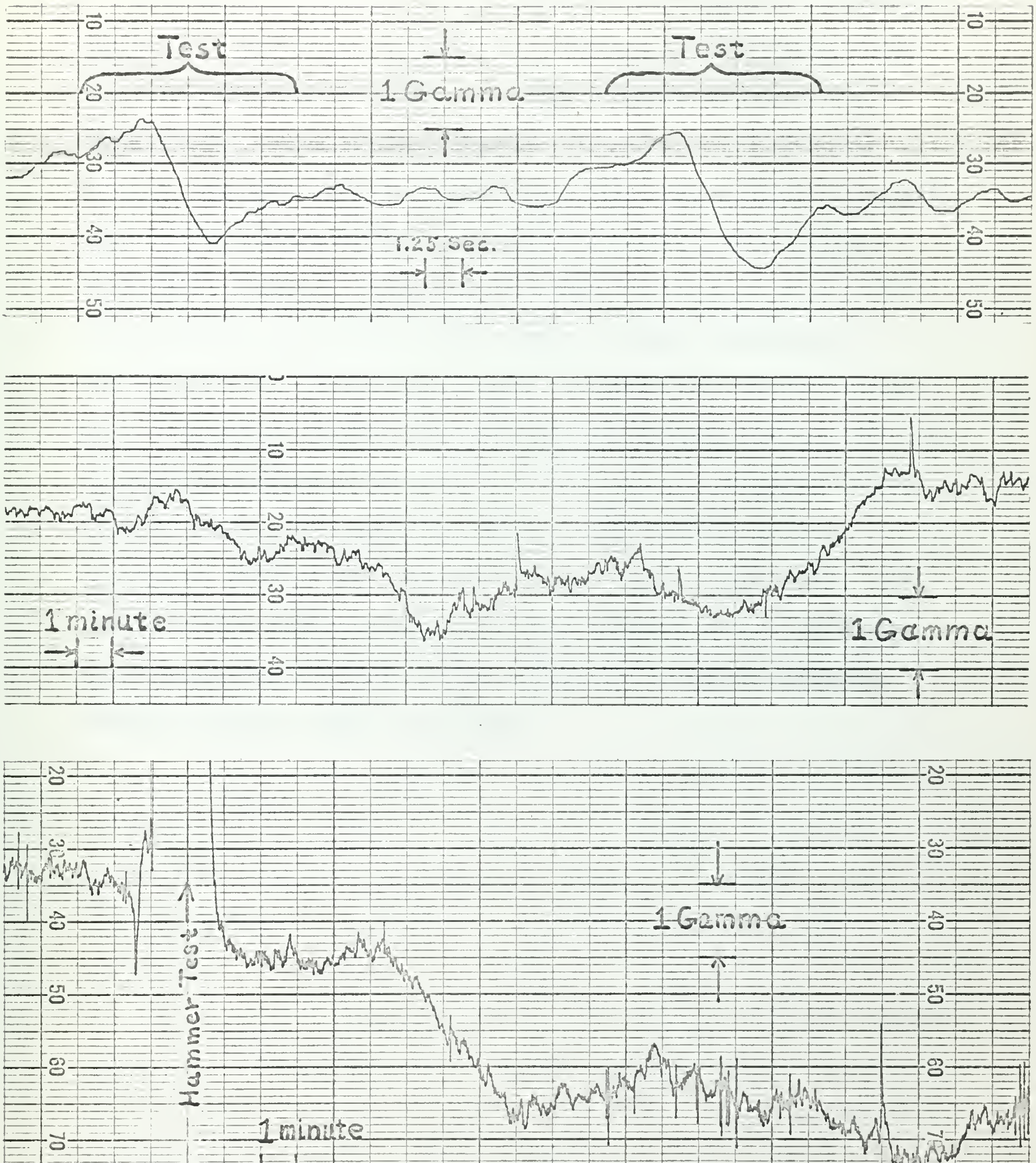

Direct Recording of Maser Oscillator Frequency

Figure 26.

To further demonstrate the advantages of the maser oscillator as a magnetometer some means of direct continuous frequency measurement is desirable. This was accomplished by generating the 23rd harmonic of the signal frequency ($\approx$ 49795 cps). This harmonic was mixed with a stable 50 KCS source and the difference frequency ($\approx$ 205 cps) was measured with an analog frequency meter. This represented the simplest means of obtaining a suitable measurement accuracy using available laboratory equipment. Recordings were made for ten gamma full scale to an accuracy of about 1% of full scale. A sample recording is shown in Fig. 26. In the upper figure two passes of a one-half pound hammer about three to four feet from the magnetometer head are indicated by derivative signal of the form 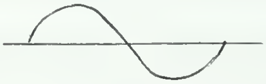 , as marked in the figure. Passing the hammer much closer to the coils resulted in driving the recorder off scale and/or loss of maser oscillation. Upon removal of the hammer, normal oscillation returned without any equipment adjustment. The lower charts in Fig. 26 are two thirty-minute records of ambient field fluctuations.

9. Conclusions.

From the results of the experiments described in this paper, several conclusions may be drawn regarding the use of dynamic polarization in nuclear resonance magnetometers. These fall into two areas, equipment and sample materials.

The modified free precession magnetometer, while valuable for observing the effects of dynamic polarization, appears to have few, if any, advantages over the standard version. The same type of signal is obtained from each, offering no improvement in either available measuring time or accuracy. The decrease in size and weight resulting from the smaller DC power supply is offset by the added weight and complexity of the radio frequency circuit. The sample that must be used is more expensive and difficult to handle than those used in the standard magnetometer.

The primary advantage of the maser oscillator is the continuous field measurement that it allows. Although it was not demonstrated experimentally, the maser oscillator inherently provides a capability for more accurate field measurement than does the free precession magnetometer. The large DC power supply and switching and timing circuits necessary in the free precession magnetometer are eliminated. They are replaced by a simple radio frequency circuit having modest power requirements.

Of the sample materials tested, results were obtained with potassium peroxylamine disulfonate alone. The only limitation on the use of this material appears to be its lifetime. While it was shown that the material could be used continuously for periods in excess of 16 hours, in a working magnetometer the material should have a useable lifetime of several months. This is particularly necessary in military applications.

Based on the above, it is felt that the advantages gained from using dynamic polarization in a nuclear resonance magnetometer of the maser oscillator type would justify an extensive research effort aimed toward discovering a suitable free-radical material.

10. Bibliography.

1. G. Breit and I. Rabbi, "Measurement of Nuclear Spin," Physical Review, Vol. 38, 2082, November,1931.

2. A. W. Overhauser, "Paramagnetic Relaxation in Metals", Phys. Rev. Vol. 89, No. 4, 689, February, 1953.

3. A. W. Overhauser, "Polarization of Nuclei in Metals", Phys. Review, Vol. 92, No. 2, 411, June, 1953.

4. Bowen, Ch. Jr. "An Earth's Field Magnetometer That Utilizes The Free Precession of Protons", Thesis, U. S. Naval Postgraduate School, 1954.

5. A. Abragam, "Overhauser Effect in Non-Metals", Phys. Rev., Vol. 98, No. 6, 1729, 1955.

6. Yowell, G. Mc. Jr. "A High Data Rate Free Precession Magnetometer", Thesis, U. S. Naval Postgraduate School, 1956.

7. T. R. Carver and C. P. Slichter, "Experimental Verification of the Overhauser Nuclear Polarization Effect", Phys. Rev. Vol. 102, No. 4, 975, 1956.

8. L. H. Bennett and H. C. Torrey, "High Negative Nuclear Polarizations in a Liquid", Phys. Review, Vol. 108, 499, 1957.

9. D. L. Cooper, "The Feasibility of the Use of Overhauser Effect in a Nuclear Free Precession Magnetometer." Thesis, U. S. Naval Postgraduate School, 1959.

10. J. Freycenon, "A Magnetometer for Measuring the Earth's Field Using Nuclear Paramagnetic Resonance with Dynamic Nuclear Polarization", L'ONDE Electrique, Vol. 40, 590-601, September, 1960.

11. B. Donnally and T. M. Sanders, Jr., "Simple Transistor Oscillator for Magnetic Resonance", Review of Scientific Instruments, Vol. 31, No. 9, 977, September, 1960.

12. J. Combrisson, "Polarization of Nuclei and Generation of Radio Frequency Energy by Nuclear Precession", Quantum Electronics, Columbia University Press, New York, 1960.

13. N. Bloemenbergen, "Nuclear Magnetic Relaxation", Frontiers in Physics, W. A. Benjamin Inc., New York, 1961.

14. A. Abragam, "The Principles of Nuclear Magnetism", Oxford University Press, 1961.

15. J. Smidt, "Magnetic and Electric Resonance and Relaxation", Proceedings of the XIth Colloque Ampere, Eindhoven, July 2-8, 1962, Wiley, 1963.

16. S. A. Al'tshuler and B. M. Koyyrev, "Electron Paramagnetic Resonance", Academic Press, New York, 1964.

APPENDIX A

Modulated Field Approach

In order to demonstrate the advantage of using the Overhauser Effect it would be desirable to operate the equipment both with and without the Overhauser Effect enhancement. In this regard the methods used should be as compatible as possible so that realistic comparisons may be made.

One method of observing nuclear resonance is the modulated field technique shown in Fig. 28. As the field is swept through the value corresponding to the particular frequency of the oscillator there is a resonant absorption in the sample coil. Near resonance the absorption varies as shown in Fig. 27.

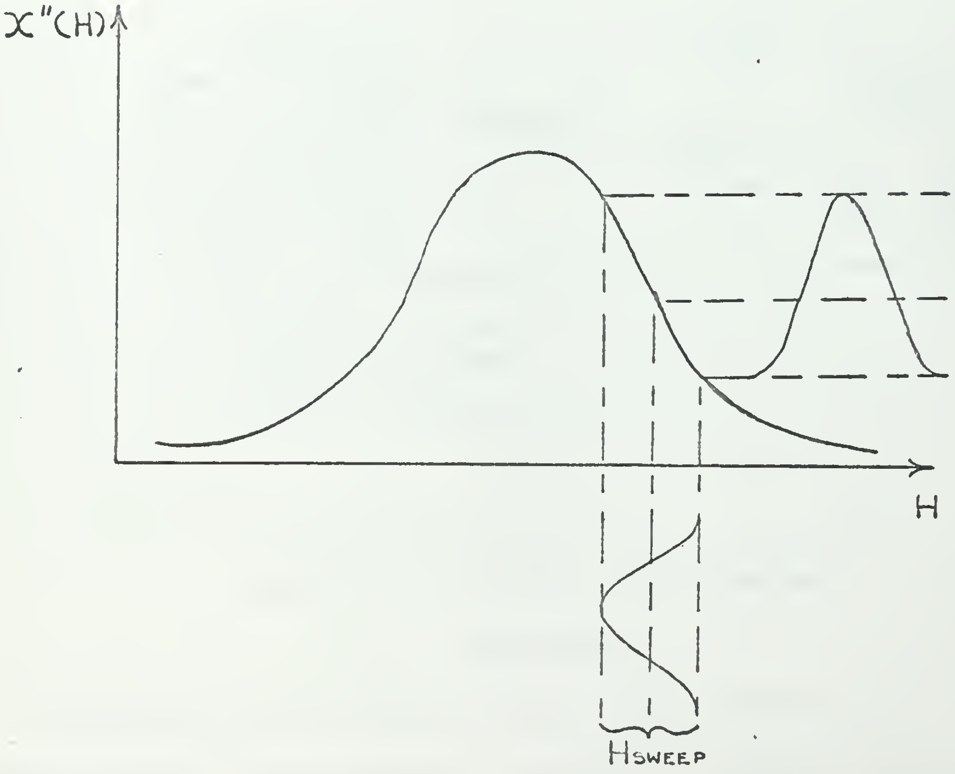

Modulated Field Absorption

Figure 27.

In the absence of the sample material there is no coupling between the sample and sweep coils which are oriented at right angles. The nuclear spins of the sample provide the only coupling between the coils. If a voltage at the nuclear resonant frequency is applied to the detection coils this signal will be amplitude modulated at the sweep frequency. The presence of the amplitude modulation is an indication of the occurrence of resonance in the sample. Where the resonant line width of the sample is wider than the field sweep then the effect of the resonant absorption is shown by Fig. 27. When the sweep field is greater than the line width then the modulation should be a replica of the resonance line. The following paragraphs describe the modulated field system shown in Fig. 28.

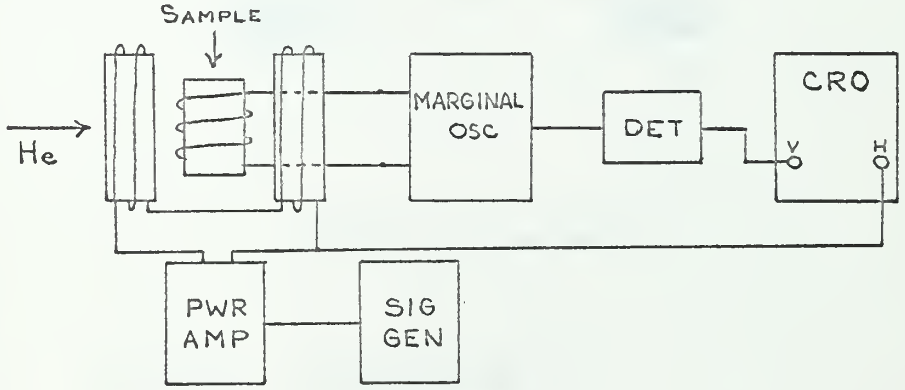

Modulated Field System Block Diagram

Figure 28.

The Helmholtz pair is used to vary the earth's field at a low frequency rate. The frequency is chosen to be slow as compared with the nuclear signal frequency of approximately 2 KC. The marginal oscillator signal period is 0.5 msec, and for a 60 cps field sweep

rate, a full trace would be completed in half the period or 8.3 msec. This sweep period covers only 16 cycles of the oscillator frequency giving little chance to average out any noise on the oscillator signal or in fact to observe a change in the amplitude. A 10 cps field sweep rate gives a 50 msec period and a more adequate 100 cycles of the signal are observed during the duration of the field sweep. For the Helmholtz coils the center field may be computed using the formula for the field induced along the axis of a circular coil.

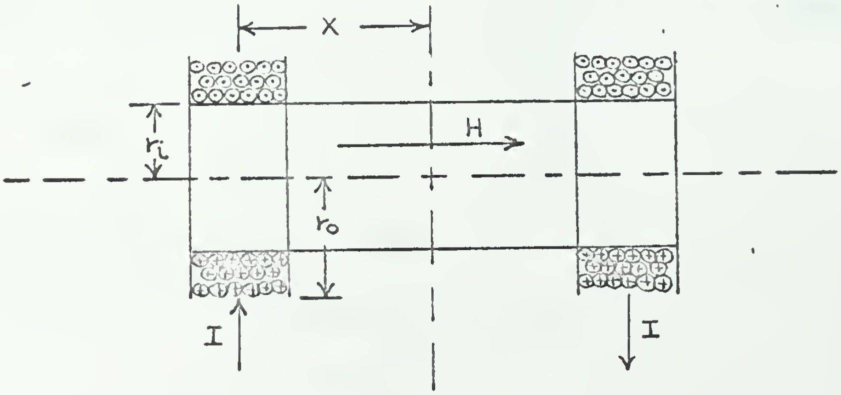

Helmholtz Sweep Coils

Figure 29.

$$\text{H center (per coil)} = \frac{N r^2 (4\pi \times 10^{-3})}{2(r^2 + x^2)^{3/2}}$$

where: $r = \left[\frac{r_i^2 + r_i r_o + r_o^2}{3}\right]^{1/2}$

For the experimental set up:

N = 100 turns per coil

r_i = .076m

r = .0891m

H = 8.42I

r_o = .1015m

x = .0572m

Assume that the maximum peak field required is 0.5 oersteds, the value of the earth's field. Then,

$$I_{max} = \frac{H}{8.42} = 59.4 \text{ ma} .$$

A laboratory signal generator may be used to drive a current generator as shown below.

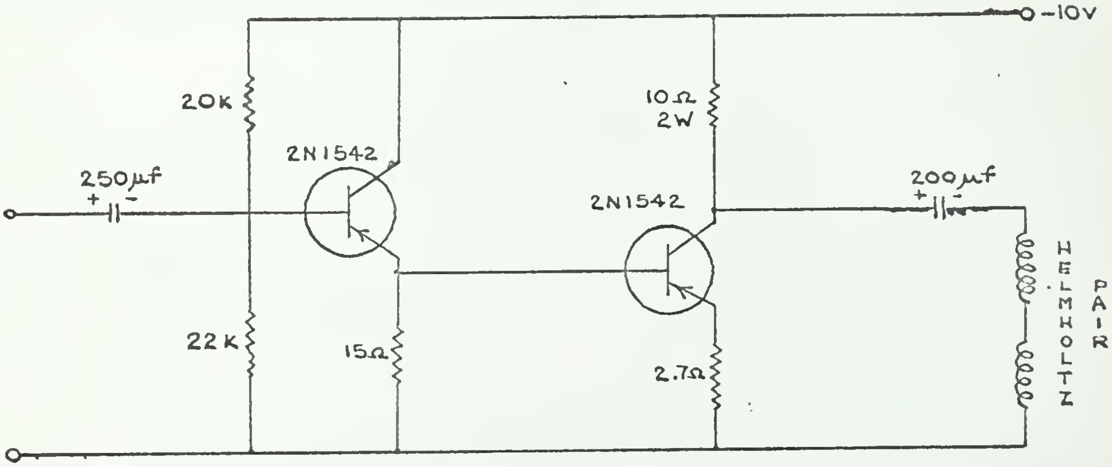

Helmholtz Coil Driver

Figure 30.

Consider the sample to be used. For water $T_1 = T_2 = 2.3$ sec. Thus a sweep rate of about 1 cps or less must be used to allow the lattice to return to equilibrium between sweeps. However, it is possible to "dope" the water sample with paramagnetic impurities thus shortening the relaxation time as well as improving the steady state signal. The line width must also be considered since, as the relaxation time is shortened, the line width increases. For maximum sensitivity a minimum line width is desirable. A pure water sample has a line width on the order of a few milligauss. The relationship between line width, sweep frequency and relaxation time may be seen from the following equation and from the considerations previously given for sweep rate.

$L =$ line width

$= 1/\gamma T_1$

For this case $\gamma = \gamma_P = 2.67528 \times 10^4 \dfrac{1}{\text{sec-oersted}}$.

To obtain such a sample as described a copper sulfate doped water was chosen. The amount of doping can be determined from Fig. 31, taken from N. Bloemenbergen's "Nuclear Magnetic Relaxation", [13] .

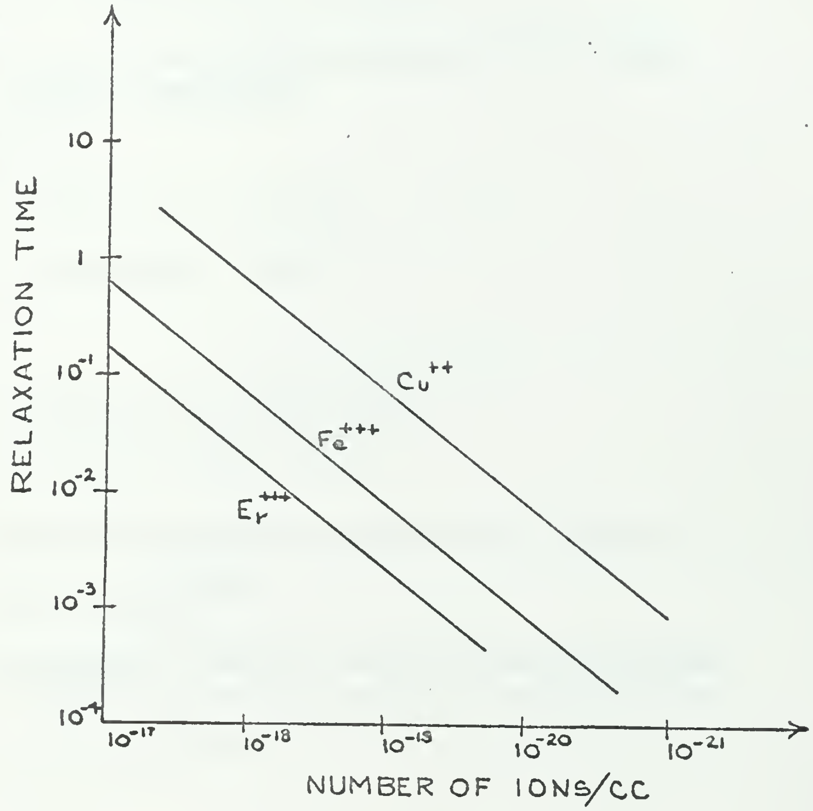

The Relaxation Time of the Proton Resonance
In Aqueous Solutions of Paramagnetic Salts

Figure 31.

Consider the effect of absorption on the tuned circuit of the marginal oscillator. Assume that the "r.f." field produces negligible saturation.

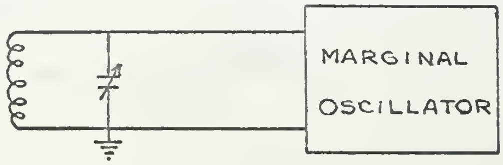

Define the following:

$\omega = 2\pi\nu$ resonant frequency

$V_c =$ volume of the coil

$\eta =$ filling factor

$L =$ inductance of the coil

$V_s =$ volume of the sample

$= \eta V_c$

$H_0 =$ the Earth's Field Intensity

$2H_1 \cos\omega t =$ "r.f." field applied across the coil by the marginal oscillator

$\epsilon\omega = \pm\omega$

where: $+ \Longrightarrow \omega_0 = -\gamma H_0 > 0$

$- \Longrightarrow \omega_0 = -\gamma H_0 < 0$

$i =$ current in the signal coil

$= I \cos\omega t = re(I e^{j\omega t})$

$\Phi =$ flux in the coil due to the "r.f." field

$= Li = L\ re(Ie^{jwt})$

$M_x =$ component of nuclear magnetization along the "r.f." field which exists only within the coil

$= re(2\chi H_1 e^{j\omega t})$

where:

$\chi =$ the complex "r.f." susceptibility which exists essentially only at resonance

$= \chi' + j\chi''$

hence:

$\vec{B} =$ the flux of the induction vector across the coil

$= \vec{H} + 4\pi\vec{M}$

$= re[L(1+4\pi\eta\chi)Ie^{j\omega t}]$

From the result for $\vec{B}$ above, the inductance in the presence of nuclear resonance may be defined as a complex quantity, i.e.

$$L_r = L(1+4\pi\eta\chi) \ .$$

The tuned circuit will develop a voltage across its terminals proportional to the parallel impedance. When external loading on the tank is negligible, this is given by

$$Z = \frac{1}{\left[\frac{1}{r+j\omega L(1+4\pi\eta\chi)} + j\omega C\right]} \ .$$

At resonance:

$$\omega = \frac{1}{\sqrt{LC}} \ , \text{ hence,}$$

$$Z = \frac{1}{R\left[\frac{1+j4\pi Q\eta\chi}{1+4\pi\eta\chi - j/Q}\right]}$$

where: $R = \frac{L^2\omega^2}{r}$ the shunt resistance of the circuit

$Q =$ the unloaded Q of the coil

$Q \gg 1$.

The quantity χ is larger than the DC susceptibility by a factor $\frac{\omega}{\Delta\omega}$ but remains a small number except in strong r.f. fields.
Since $Q \gg 1$, the impedance becomes

$$Z = R\left[1 - j4\pi Q\chi\right]$$

$$= R\left[1 - 4\pi\eta Q(\chi'' + j\chi')\right] .$$

When the earth's field is swept through resonance there is a relative change in Z and hence a relative change in voltage given by

$$\frac{\delta V}{V} = j\,4\pi \eta Q \chi \,,$$

and for , the relative amplitude change is

$$\left| 1 - jQ\,4\pi\eta\chi \right| - 1$$

$$\approx -4\pi\eta Q \chi''$$

The susceptibility in the absence of an "r.f." field is

$$\chi_0 = \frac{n I (I+1) \mu_n^2}{3 I^2 k T}$$

$$= 3.41 \times 10^{-10} (\text{GAUSS})^{-1} \text{ for protons.}$$

The complex susceptibility is given by

$$\chi''(\omega) = \pi/2\, (\chi_0 \omega_0 f(\omega) \,.$$

Assume the resonance line has a Lorentzian shape, then

$$f(\omega) = \frac{T}{\pi} \frac{1}{1 + (\omega - \omega_0)^2 T_2^2} \,.$$

Define Δ = the half width at half intensity

= $1/T_2$.

Substituting gives

$$\chi''(\omega_0) = \frac{1}{2} \omega_0 T_2 \chi_0 = \frac{\chi_0 \omega_0}{2\Delta}$$

$$\frac{\delta V}{V} = -2\pi\eta Q \omega_0 T_2 \chi_0 \,.$$

This equation shows the disadvantage of performing the experiment at low fields. The factors χ_0, T_2, and η are functions of the material and coil arrangement. The sensitivity is thus determined by the frequency, recall $\omega_0 = \gamma_p H$ and Q is proportional to ω. High Q circuits are notably easier to obtain as the frequency goes up. For the particular arrangement chosen for this experiment

$$\frac{\delta V}{V} = -6.13 \times 10^{-4} T_2 \ .$$

Recall that a short T_2 is desired to allow adequate spin relaxation between field sweeps, or a very slow sweep must be utilized. In any case the sensitivity in low fields is very poor.

APPENDIX B

Sample Preparation

The following paragraphs describe the preparations and handling of the various samples used in the experiments discussed in Sections 7 and 8.

1. Potassium Peroxylamine Disulfonate, $K_2(SO_3)_2NO$

The sample used was a .01 molar solution in 250 ml of doubly-distilled, dust-free water. The distilled water was placed in the sample container and the pH was adjusted to 9-10 with sodium hydroxide, NaOH. At room temperature the strength of an unadjusted solution will decay rapidly. The $K_2(SO_3)_2NO$ powder was then added to the distilled water and the solution deoxygenated by bubbling nitrogen gas through it. The container was then sealed to make it airtight. If properly handled when in use, the sample should be useable for several days. Decay of the sample is indicated by a change in color from light purple to clear. When not in use, the sample should be refrigerated or frozen.

2. 2,2 - Diphenyl - 1 - Picrylhydrazyl (DPPH), $(NO_2)_3C_6H_2NN(C_6H_5)_2$

The sample used was a .01 molar solution in 250 ml of benzene. A solution of DPPH in benzene will decompose rapidly in the presence of oxygen. Therefore, the benzene was first placed in the sample container and deoxygenated by bubbling nitrogen gas through it. The DPPH crystals were then added to the benzene and the glass container sealed, making it airtight. The sample should be kept refrigerated when not in use.

3. Benzophenone and Sodium in Tetrahydrofuran

This sample requires great care in preparation or the solution will decay rapidly. The Tetrahydrofuran (THF) was first dried over calcium hydride, CaH_2, separated from the CaH_2, and distilled. Nitrogen

gas was bubbled through the THF to deoxygenate it. Benzophenone was then added to make a .2 molar solution. Small pieces of freshly cut sodium were then added to the solution of THF and benzophenone. The reaction was complete in approximately an hour. 100 ML of dry THF were placed in each sample container and 20 ML of the solution were added to each container. The resulting solution was dark blue in color and had about a .02 molar concentration. Again, when not in use, the sample should be refrigerated.

APPENDIX C

Equipment Circuit Diagrams

This appendix contains the circuit diagrams for the equipment constructed for use in the maser oscillator.

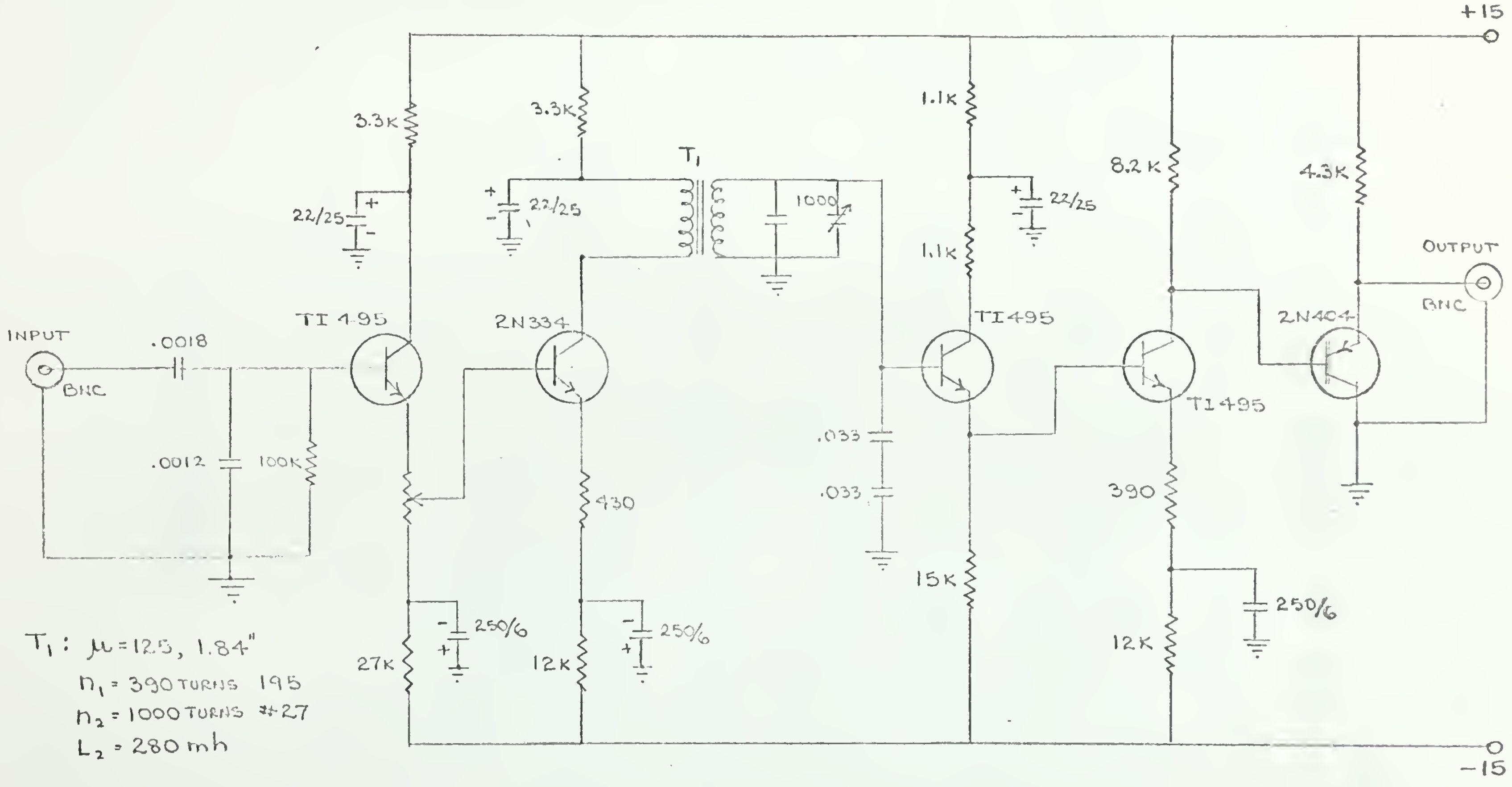

T_1 : $\mu = 125$, 1.84"
n_1 = 390 TURNS 195
n_2 = 1000 TURNS #27
L_2 = 280 mh

CIRCUIT DIAGRAM
2 KC BANDPASS AMPLIFIER

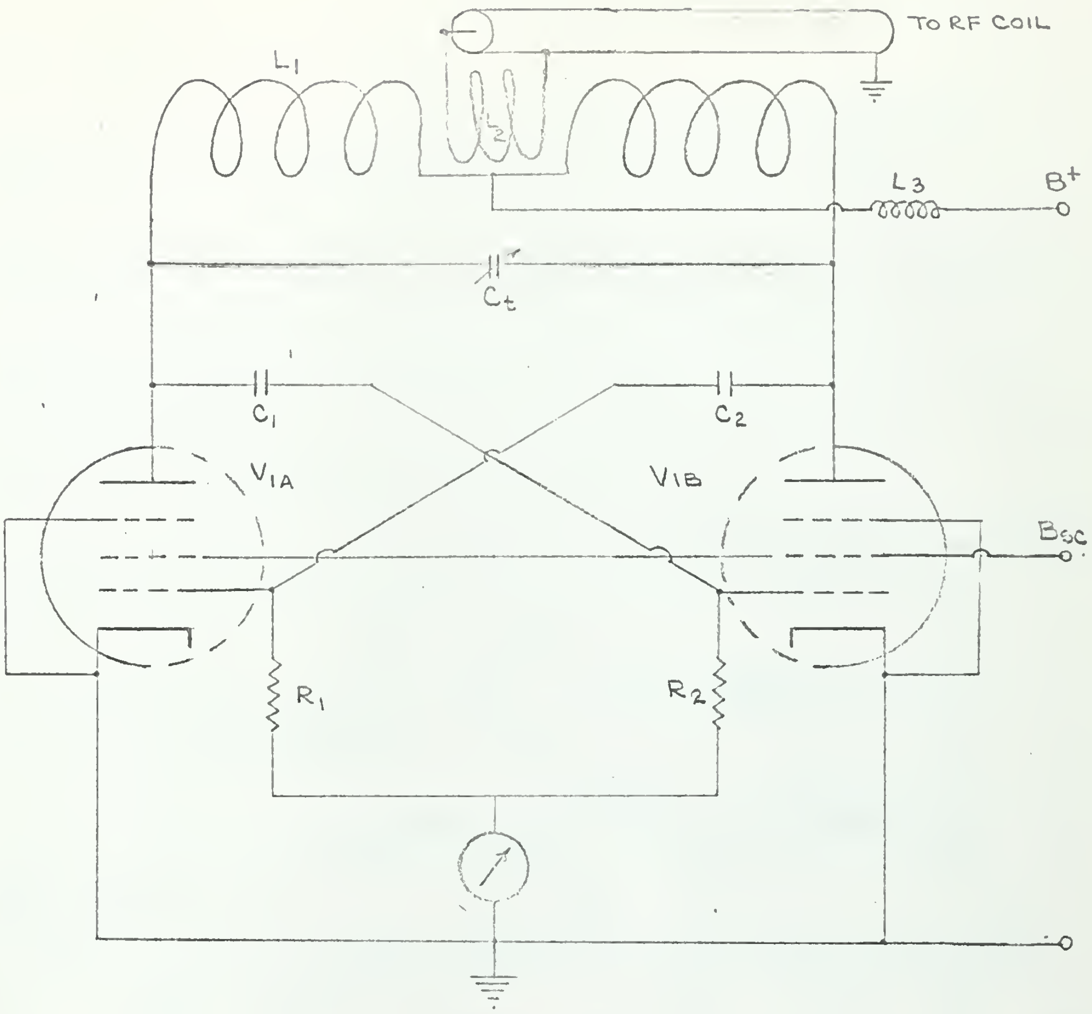

$C_1 = C_2 = 22$ pf

C_t = TUNING CAPACITOR

B^+ = 500 VDC

B_{SC} = 250 VDC

V_1 — 829B

L_1 = 5 TURNS #6 WIRE I.D. 1 1/16"

L_2 = 2 TURNS #12 WIRE I.D. 1 1/16"

L_3 = R.F. CHOKE

$R_1 = R_2$ = 20K, 1 WATT

CIRCUIT DIAGRAM
R.F. OSCILLATOR

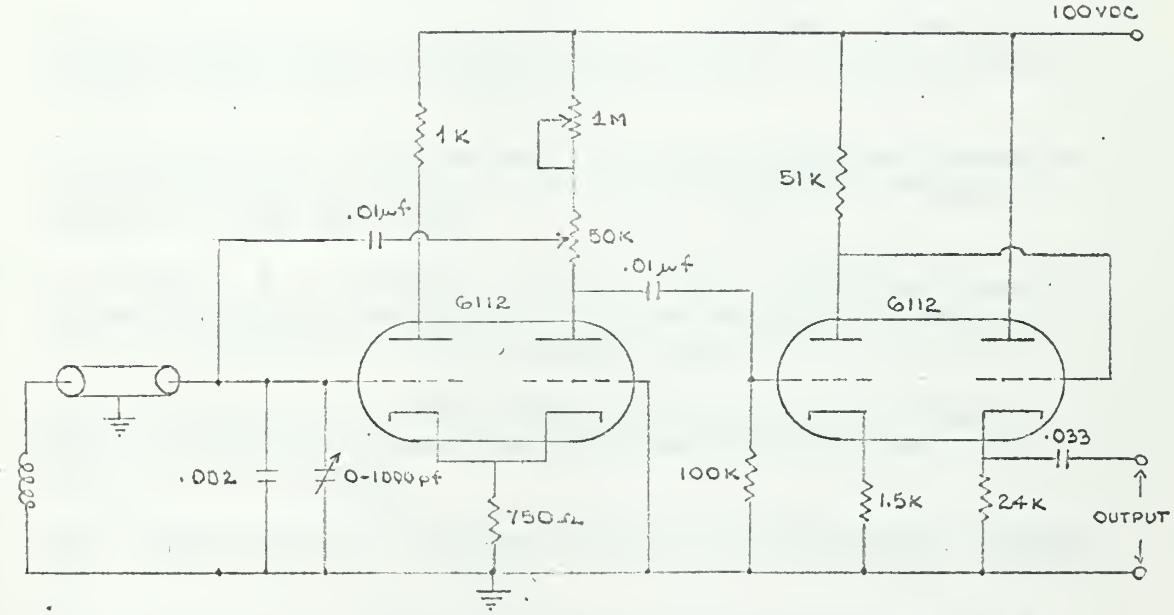

CIRCUIT DIAGRAM
MARGINAL OSCILLATOR AND AMPLIFIER

APPENDIX D

Subsidiary Bibliographical Material

1. N. Bloemenbergen, E. M. Purcell, and P. V. Pound, "Relaxation Effects in Nuclear Magnetic Resonance Absorption", Physical Review, Vol. 73, No. 7, April 1, 1948.

2. J. E. Nafe and E. B. Nelson, "The Hyperfine Structure of Hydrogen and Deuterium", Physical Review, Vol. 73, No. 7, April 1, 1948.

3. F. Bloch, "Nuclear Induction", Physical Review Vol. 70, No. 7 & 8, October 1-15, 1948.

4. F. Bloch, "The Nuclear Induction Experiment," Physical Review, Vol. 70, No. 7 & 8, October 1-15, 1948.

5. C. A. Hutchinson, R. C. Pastor and A. G. Kowalski, "Paramagnetic Resonance Absorption in Organic Free Radicals. Fine Structure", J. Chem. Phys., Vol. 20, 534, 1952.

6. J. Townsend, S. I. Weissman and G. E. Pake, "Hyperfine Structure in the Paramagnetic Resonance of the Ion $(SO_3)NO^{--}$", Physical Review, Vol. 85, 682, 1952.

7. J. Townsend, S. I. Weissman, and G. E. Pake, "Hyperfine Structure in the Paramagnetic Resonance of the Ion $(SO_3)_2NO^{--}$", Physical Review, Vol. 89, No. 3, 606, February 1953.

8. J. P. Lloyd and G. E. Pake, "Spin Relaxation in Free Radical Solutions Exhibiting Hyperfine Structure", Physical Rev., Vol. 94, No. 3, May 1, 1954.

9. C. H. Townes and A. L. Schawlow, "Microwave Spectroscopy", McGraw Hill Book Co., New York, 1955.

10. W. A. Barker, "The Overhauser Effect in Paramagnetic Systems", Argonne National Laboratory, ANL-6069, November, 1959.

11. A. Abragam, J. Combrisson and I. Solomon, "Nuclear Polarization By Overhauser Effect in Solutions of Paramagnetic Ions", Academie Des Sciences, C. R. V. 245; No. 2, 157-160, 8 July 1957.

12. A. Landesmon, "Nuclear Resonance Signals Obtained By Dynamic Polarization", Academie Des Sciences, C.R.V. 246, No. 10, 1538-1840, March 10, 1958.

13. R. V. Pound and R. Freeman, "Frequency Control of an Oscillator by Nuclear Magnetic Resonance". Review of Scientific Instruments, Vol. 31, No. 2, 96-102, 1960.

14. R. Freeman and R. V. Pound, "High-Resolution NMR Spectrometer with Radio-Frequency Controlled by the Magnetic Field". Ibid 103-106, 1960.

15. R. H. Webb, "Steady-State Nuclear Polarizations via Electronic Transitions", Am. J. Phys., 29, 428-444, 1961.

16. F. N. H. Robinson, "Frequency Modulated NMR Oscillator Without Amplitude Modulation". Review of Scientific Instruments, Vol. 34, No. 11, 1260, November 1963.

17. C. P. Slichter, "Principles of Magnetic Resonance", Harper and Row, 1963.

18. A. Timar, I. Fatt, and R. C. LaForce, "Frequency-stable Nuclear-Magnetic Resonance Absorption Circuit for Small Filling Factors". Review of Scientific Instruments, Vol. 35, No. 5, 1224-1225, September 1964.

thesB855
The application of dynamic polarization
3 2768 002 07924 6
DUDLEY KNOX LIBRARY